THE JOURNAL OF BIOLOGICAL CHEMISTRY VOL. 289, NO. 10, pp. 6809–6824, March 7, 2014

Phosphatidylethanolamine Synthesis in the Parasite Mitochondrion Is Required for Efficient Growth but Dispensable for Survival of *Toxoplasma gondii*[*]

Received for publication, August 13, 2013, and in revised form, January 14, 2014 Published, JBC Papers in Press, January 15, 2014, DOI 10.1074/jbc.M113.509406

Anne Hartmann[‡], **Maria Hellmund**[‡], **Richard Lucius**[‡], **Dennis R. Voelker**[§], **and Nishith Gupta**[‡¶1]

From the [‡]*Department of Molecular Parasitology, Humboldt University, Philippstrasse 13, 10115 Berlin, Germany, the* [§]*Department of Medicine, National Jewish Health, Denver, Colorado 80206, and the* [¶]*Department of Parasitology, Max-Planck Institute for Infection Biology, Charitéplatz 1, 10117 Berlin, Germany*

Background: *Toxoplasma gondii* is a common intracellular parasite of diverse host cells.
Results: The parasite can produce phosphatidylethanolamine in its mitochondrion, endoplasmic reticulum, and parasitophorous vacuole, which together allow versatile lipid biogenesis.
Conclusion: Multiple routes of lipid synthesis ensure parasite survival in discrete nutrient milieus.
Significance: *T. gondii* offers an instructive model to study membrane biology of parasitic protists.

***Toxoplasma gondii* is a highly prevalent obligate intracellular parasite of the phylum Apicomplexa, which also includes other parasites of clinical and/or veterinary importance, such as *Plasmodium*, *Cryptosporidium*, and *Eimeria*. Acute infection by *Toxoplasma* is hallmarked by rapid proliferation in its host cells and requires a significant synthesis of parasite membranes. Phosphatidylethanolamine (PtdEtn) is the second major phospholipid class in *T. gondii*. Here, we reveal that PtdEtn is produced in the parasite mitochondrion and parasitophorous vacuole by decarboxylation of phosphatidylserine (PtdSer) and in the endoplasmic reticulum by fusion of CDP-ethanolamine and diacylglycerol. PtdEtn in the mitochondrion is synthesized by a phosphatidylserine decarboxylase (*Tg*PSD1mt) of the type I class. *Tg*PSD1mt harbors a targeting peptide at its N terminus that is required for the mitochondrial localization but not for the catalytic activity. Ablation of *Tg*PSD1mt expression caused up to 45% growth impairment in the parasite mutant. The PtdEtn content of the mutant was unaffected, however, suggesting the presence of compensatory mechanisms. Indeed, metabolic labeling revealed an increased usage of ethanolamine for PtdEtn synthesis by the mutant. Likewise, depletion of nutrients exacerbated the growth defect (~56%), which was partially restored by ethanolamine. Besides, the survival and residual growth of the *Tg*PSD1mt mutant in the nutrient-depleted medium also indicated additional routes of PtdEtn biogenesis, such as acquisition of host-derived lipid. Collectively, the work demonstrates a metabolic cooperativity between the parasite organelles, which ensures a sustained lipid synthesis, survival and growth of *T. gondii* in varying nutritional milieus.**

Toxoplasma gondii is an obligate intracellular parasite that causes cerebral and ocular toxoplasmosis in immunosuppressed individuals as well as congenital disease and abortions in animals and humans. It can infect and replicate in nearly all nucleated vertebrate cells and thus poses a major threat to global health. Besides that, the parasite serves as a model organism to understand the biology of parasitic and free living protozoa. Successful infection and transmission of *T. gondii* depends on the interconversion between its fast replicating tachyzoite and dormant bradyzoite stages. The lytic cycle begins with the infection of host cells by tachyzoites, which cause tissue necrosis and acute infection (1). Upon immune and physicochemical stress (pH, temperature, etc.), tachyzoites convert into bradyzoite-containing cysts (chronic infection) (2). Such cysts are commonly formed in the neural and muscular tissues and persist for the entire life of the infected host (2).

The promiscuous parasitism of *T. gondii* in assorted niches necessitates a discretionary access to host resources and fine tuning of the parasite's metabolism. The parasite resides in a parasitophorous vacuole, which provides a safe environment and interface for acquisition of nutrients. The rapid replication of intracellular tachyzoites and concomitant expansion of the parasitophorous vacuole are accompanied by significant membrane synthesis and nutritional import from the host cell (3). Similar to other eukaryotes, phospholipids account for a major fraction of parasite membranes, which include phosphatidylcholine (PtdCho),[2] PtdEtn, phosphatidylinositol, and PtdSer

[*] This work was supported by German Research Foundation (Deutsche Forschungsgemeinschaft; DFG) Grants SFB618/C7 and GU1100/3-1 (to N. G.) and by a 6-month scholarship from the Caroline von Humboldt Foundation (to A. H.).

[1] To whom correspondence should be addressed: Dept. of Molecular Parasitology, Humboldt University, Philippstrasse 13, 10115 Berlin, Germany. Tel.: 49-30-20936404; Fax: 49-30-20936051; E-mail: Gupta.Nishith@staff.hu-berlin.de.

[2] The abbreviations used are: PtdCho, phosphatidylcholine; PtdEtn, phosphatidylethanolamine; PtdSer, phosphatidylserine; ATc, anhydrotetracycline; Der1, degradation in the endoplasmic reticulum protein 1; DHFR-TS, dihydrofolate reductase thymidylate synthase; EPT, CDP-ethanolamine: diacyglycerol ethanolamine-phosphotransferase; F1B, ATPase subunit F1-β; Gap45, gliding-associated protein (45 kDa); GRA2, dense granule protein 2; HFF, human foreskin fibroblast(s); Hsp90, heat-shock protein (90 kDa); HXGPRT, hypoxanthine xanthine guanine phosphoribosyltransferase; IT, insertional tagging; mt, mitochondrion; MOI, multiplicity of infection; PSD, phosphatidylserine decarboxylase; pv, parasitophorous vacuole; Scr, screening; TLC, thin layer chromatography; UPRT, uracil phosphoribosyltransferase; UPKO, UPRT knock-out; ER, endoplasmic reticulum; gDNA, genomic DNA.

(4). *T. gondii* has the potential to synthesize its major phospholipids (4–6) and harbors a relatively complete set of enzymes for *de novo* synthesis (4, 5). Unlike PtdCho and PtdSer, for which the parasite harbors only one route, PtdEtn is made by decarboxylation of PtdSer and by the CDP-ethanolamine pathway (4). The physiological relevance of *de novo* phospholipid syntheses in *T. gondii* remains to be understood, however.

PtdEtn is one of the most abundant phospholipids in prokaryotes and eukaryotes, which contributes to the membrane integrity, membrane fusion/fission, protein stabilization, and autophagy events (7). It is enriched in the mitochondrial membrane and can be made by PtdSer decarboxylation and/or the CDP-ethanolamine pathway (8). PtdSer decarboxylase (PSD) enzymes are a unique subgroup of decarboxylases, which carry a pyruvoyl group at their active site (9). Bacteria and mammalian cells express a single PSD protein, whereas two to three distinct PSDs have been identified in yeast and plants, respectively (10–12). Quite notably, *T. gondii* tachyzoites display a much higher (10-fold) PSD activity when compared with yeast and mammalian cells (4). We have shown that the PSD activity in *T. gondii* comprises membrane-bound and soluble fractions (13). The PSD attributed to the soluble activity is secreted/excreted into the parasitophorous vacuole (*Tg*PSD1pv) via dense granules (13), whereas the other PSD has, so far, remained elusive. This study aimed to (*a*) characterize the membrane-associated PSD for its activity and subcellular location, (*b*) determine its relative importance for PtdEtn synthesis, and (*c*) examine the cooperativity of distinct routes of PtdEtn synthesis for membrane biogenesis, survival, and growth of *T. gondii*, if any.

MATERIALS AND METHODS

Biological Reagents and Resources—Cell culture chemicals were purchased from PAA, Biowest, and Biochrom. Other standard reagents were procured from AppliChem, Carl Roth, and Invitrogen. Anhydrotetracycline (ATc) was from IBA Lifesciences. L-[1-^{14}C]Serine, L-[1-^{3}H]serine, and L-[1,2-^{14}C]ethanolamine were from ICN Radiochemicals and American Radiolabeled Chemicals. RNA purifications, first strand cDNA syntheses, and DNA isolations were performed using commercial kits from Invitrogen and Analytik Jena. DNA-modifying enzymes were from New England Biolabs (Germany). Silica gel 60 plates for thin layer chromatography (TLC) were obtained from Merck-Millipore. Lipid standards were procured from Avanti Polar Lipids. Primary (α-HA) and Alexa488/594-conjugated secondary antibodies as well as oligonucleotides were supplied by Sigma-Aldrich and Invitrogen, respectively. Anti-*Tg*Gap45 (14), anti-*Tg*F1B (15), and *Tg*Hsp90 antibodies were provided by Dominique Soldati-Favre (University of Geneva), Peter Bradley (University of California), and Sergio Angel (IIB-INTECH, Argentina), respectively. The Δ*ku80-TaTi* (16) and Δ*ku80-hxgprt*$^{-}$ (17) strains (type I) of *T. gondii* were provided by Boris Striepen (University of Georgia) and Vern Carruthers (University of Michigan). The *pTKO* plasmid and *Tg*Der1-GFP (18) construct were donated by John Boothroyd (Stanford University) and Boris Striepen, respectively. The *Saccharomyces cerevisiae* mutant (*psd1*Δ*psd2*Δ, BY23480) was obtained from Akio Toh-e (Chiba University).

Parasite Culture and Expression Constructs—Human foreskin fibroblasts (HFF; Cell Line Service) were cultured in Dulbecco's modified Eagle's medium (DMEM) supplemented with 10% fetal calf serum (FCS), 2 mM glutamine, minimum essential medium (MEM) non-essential amino acids, 100 units/ml penicillin, and 100 μg/ml streptomycin at 37 °C and 5% CO_2 in a humidified incubator. Tachyzoites (Δ*ku80-TaTi* and Δ*ku80-hxgprt*$^{-}$) were maintained by serial passage in HFF monolayers at a multiplicity of infection (MOI) of 3. Parasite RNA was isolated using TRIzol and reverse-transcribed into first-strand cDNA. The open reading frames (ORFs) of *Tg*PSD1mt, *Tg*PSD1pv, and *Tg*EPT1/2 were amplified from cDNA using PfuUltra II Fusion polymerase (Agilent Technologies). Primers used for PCRs are listed in Table 1.

Full-length *Tg*PSD1mt or its truncated forms (residues 91–427 and 113–427) with a C-terminal HA-tag were ligated into the *pTETO7SAG1-UPKO* plasmid at NcoI/PacI restriction sites using T4 ligase and transformed into *Escherichia coli* XL-1b for molecular cloning and vector preparation. The use of the *TETO7SAG1* promoter in the *TaTi* strain of *T. gondii* permits a tetracycline-regulatable expression of the genes (19). The ORFs of *Tg*EPT1/2-HA were cloned into the *pTgGRA2-UPKO* plasmid using NsiI and PacI sites. The *Tg*PSD1pv-HA construct in the *pTgPSD1pv-UPKO* vector was made in three sequential steps by cloning *Tg*PSD1pv-5′-UTR, *Tg*PSD1pv-HA ORF, and *Tg*NTP3–3′-UTR. The 5′-UTR of *Tg*PSD1pv (2 kb) along with the first 52 bp of the ORF was cloned using EcoRV and MscI in the *UPKO* vector. In the second step, the partial ORF (53–2904 bp) containing a C-terminal HA tag was cloned at the MscI and PacI restriction sites. Finally, the 3′-UTR of the *TgNTP3* gene was inserted using PacI and NotI (primers in Table 1). Bacterial clones were confirmed by PCR and sequencing.

Generation of Transgenic Parasite Lines—The plasmid constructs were transfected into fresh extracellular tachyzoites (Δ*ku80-TaTi* or Δ*ku80-hxgprt*$^{-}$) suspended in Cytomix (10 mM K_2HPO_4/KH_2PO_4, 25 mM HEPES, 120 mM KCl, 5 mM $MgCl_2$, 0.15 mM $CaCl_2$, 2 mM EGTA, 5 mM glutathione, 5 mM ATP, pH 7.6) using the BTX electroporation instrument (50 μg of DNA, ~10^7 parasites, 2 kV, 50 ohms, 25 microfarads, 250 μs). All *UPKO*-based vectors allow a targeted insertion of the ORF of interest at the *TgUPRT* (uracil phosphoribosyltransferase) locus following a selection by 5-fluoro-2′-deoxyuridine (20). Parasites with a disrupted *UPRT* gene locus were selected by 5 μM 5-fluoro-2′-deoxyuridine. Transgenic tachyzoites were transformed with the *Tg*Der1-GFP construct (18) for localization studies or with the *Tg*PSD1mt knock-out construct to make a conditional mutant.

The knock-out vector used to generate a conditional mutant contained the 5′- and 3′-UTR of the *TgPSD1mt* gene flanking a dihydrofolate reductase thymidylate synthase selection marker (*pTKO-TgPSD1mt-5′UTR-DHFR-TS-TgPSD1mt-3′UTR*). The UTRs were amplified from tachyzoite gDNA using the indicated primers (Table 1). The 5′-UTR (1 kb) and 3′-UTR (1 kb) were cloned into XcmI/SpeI and HpaI/ApaI restriction sites, respectively. The knock-out plasmid was transfected into the 5-fluoro-2′-deoxyuridine-resistant parasites of the Δ*ku80-TaTi* strain expressing an ectopic copy of tetracycline-regulatable *Tg*PSD1mt-HA_r, and selected with 1 μM pyrimethamine

TABLE 1
Oligonucleotides used in this study

Primer Name (restriction site)	Nucleotide Sequence (restriction site underlined)	Cloning Vector (research objective)
Expression of *Tg*PSD1mt-HA, *Tg*PSD1mt$_{(91-427)}$-HA und *Tg*PSD1mt $_{(113-427)}$ in *T. gondii* (Δ*ku80-hxgprt* and Δ*ku80-TaTi strains*)		
*Tg*PSD1-IT-F (XcmI)	CTCATCCCACCGGTCACCTGGGAGCCATGTGGCAGATATTC	*pTKO-HXGPRT* (3'HA-tagging of the *TgPSD1mt* gene locus)
*Tg*PSD1-IT-HA-R (HpaI)	CTCATCCAATTGTCAAGCGTAATCTGGAACATCGTATGGGTA GTAAAATGCAAACAGGCGTTC	
*Tg*PSD1mt$_{(91-427)}$-F (NcoI)	CTCATCCCATGGTTGGCATGACCGCG	*pTETO7SAG1-UPKO* (Ectopic expression of *Tg*PSD1mt$_{(91-427)}$ at the *TgUPRT* gene locus)
*Tg*PSD1mt$_{(91-427)}$-HA-R (PacI)	CTCATCTTAATTAATCAAGCGTAATCTGGAACATCGTATGGG TAGTAAAATGCAAACAGGCGTTCATCTT	
*Tg*PSD1mt$_{(113-427)}$-F (NcoI)	CTCATCCCATGGCGACAG ACAATGTTGCAGA	*pTETO7SAG1-UPKO* (Ectopic expression of *Tg*PSD1mt$_{(113-427)}$ at the *TgUPRT* gene locus)
*Tg*PSD1mt$_{(113-427)}$-HA-R (PacI)	CTCATCTTAATTAATCAAGCGTAATCTGGAACATCGTATGGG TAGTAAAATGCAAACAGGCGTTC	
Expression of *Tg*PSD1pv-HA in *T. gondii* (Δ*ku80-TaTi strain*)		
*Tg*PSD1pv-5'UTR-F (EcoRV)	CTCATCGATATCTGAAGGGAAGAAGCGAAGG	*pUPKO* (Cloning of the *TgPSD1pv* gene promoter)
*Tg*PSD1pv-5'UTR-R (MscI)	CTCATCTGGCCACCAGGGCCACGCACAC	
*Tg*PSD1pv-F (MscI)	CTCATCTGGCCATTTCGGTACCAGCAGCGT	*pUPKO* (Cloning of the *Tg*PSD1pv-HA ORF)
*Tg*PSD1pv-HA-R (PacI)	CTCATCTTAATTAATCAAGCGTAATCTGGAACATCGTATGGG TAGTAAAATGCAAACAGGCGTTCA	
*Tg*NTP3-3'UTR-F (PacI)	CTCATCTTAATTAAAATGTCGATTGATGGTGTCG	*pUPKO* (Cloning of the *Tg*NTP3-3´UTR)
*Tg*NTP3-3'UTR-R (NotI)	CTCATCGCGGCCGCACTAGTGTGGCGCCACGG	
Expression of *Tg*PSD1mt, *Tg*PSD1mt$_{(113-427)}$ and *Sc*PSD1 in *S. cerevisiae* (BY23480 or PTY44 strain)		
*Tg*PSD1mt-F (NotI)	CTCATCGCGGCCGCATGCGCAGTTACTTGCGGT	*pESC-Ura* (Ectopic expression of *Tg*PSD1mt ORF)
*Tg*PSD1mt-R (NotI)	CTCATCGCGGCCGCTCAGTAAAATGCAAACAGGCGT	
*Tg*PSD1mt$_{(113-427)}$-F (BglII)	CTCATCAGATCTATGGCGACAGACAATGTTGCAGAGAT	*pYES2.1* (Ectopic expression of *Tg*PSD1mt$_{(113-427)}$ ORF)
*Tg*PSD1$_{(113-427)}$-R (EcoRI)	CTCATCGAATTCTCAGTAAAATGCAAACAGGC	
*Sc*PSD1-F (NotI)	CTCATCGCGGCCGCATGTCAATTATGCCAGTTAAGAACG	*pESC-Ura* (Ectopic expression of *Sc*PSD1 ORF)
*Sc*PSD1-R (NotI)	CTCATCGCGGCCGCTCATTTTAAATCATTCTTTCCAATT	
Making of the Δ*tgpsd1mt/Tg*PSD1mt-HA$_r$ mutant in *T. gondii* (Δ*ku80-TaTi* strain)		
*Tg*PSD1-5´UTR-F1 (XcmI)	CTCATCCCACCGGTCACCTGGACTTCTTCAGCACATCGTGTGT	*pTKO-DHFR-TS* (Cloning of the *Tg*PSD1mt-5´UTR)
*Tg*PSD1-5´UTR-R1 (SpeI)	CTCATCACTAGTGCAAACATCTCAAGAGAAGCAC	
*Tg*PSD1-3´UTR-F1 (HpaI)	CTCATCGTTAACTTTGACTGAATCGCTTTGTTG	*pTKO-DHFR-TS* (Cloning of the *Tg*PSD1mt-3´UTR)
*Tg*PSD1-3´UTR-R1 (ApaI)	CTCATCGGGCCCACAGCGAAACCCCTTCAG	
Screening for 5' and 3' recombination in the Δ*tgpsd1mt/Tg*PSD1mt-HA$_r$ mutant of *T. gondii*		
*Tg*PSD1- 5´Scr-F1	GCGAGCAGGGACTAAGTGG	*pDrive* (TA-cloning of 5' PCR product for sequencing)
*Tg*PSD1-5´Scr-R1	CACAGTCTCACCTCGCCTTG	
*Tg*PSD1-3´Scr-F1	CGGAAAGTGCTTACATCGAAC	*pDrive* (TA-cloning of 3' PCR product for sequencing)
*Tg*PSD1-3´Scr-R1	GACCGACGGCAGTATGTTG	
Making of Δ*tgpsd1mt* mutant in *T. gondii* (Δ*ku80-hxgprt* strain)		
*Tg*PSD1-5´UTR-F2 (KpnI)	CTCATCGGTACCTCTGAAACCGGTTACAGACCA	*pTKO-HXGPRT* (Cloning of the *Tg*PSD1mt-5´UTR)
*Tg*PSD1-5´UTR-R2 (XhoI)	CTCATCCTCGAGCTCTGGAAGCCATAACTAGAGAAACA	
*Tg*PSD1-3´UTR-F2 (HpaI)	CTCATCGTTAACTCATGCACATGGTTGCTGTG	*pTKO-HXGPRT* (Cloning of the *Tg*PSD1mt-3´UTR)
*Tg*PSD1-3´UTR-R2 (ApaI)	CTCATCGGGCCCAACCAATGGTCGACGAAGC	
Screening for 5' and 3' recombination in the Δ*tgpsd1mt* mutant of *T. gondii*		
*Tg*PSD1- 5´Scr-F2	CGGTTTCTTTGTCGTATTCCC	*pDrive* (TA-cloning of 5' PCR product for sequencing)
*Tg*PSD1-5´Scr-R2	GACGCAGATGTGCGTGTATC	
*Tg*PSD1-3´Scr-F2	ACTGCCGTGTGGTAAAATGAA	*pDrive* (TA-cloning of 3' PCR product for sequencing)
*Tg*PSD1-3´Scr-R2	GAAAGGAGTGAAGGAGCCTATCA	
Expression of putative *Tg*EPT1-HA and *Tg*EPT2-HA in *T. gondii* (Δ*ku80-TaTi strain*)		
*Tg*EPT1-F (NsiI)	CTCATCATGCATATGATGGTCGGTGGCGT	*pTgGRA2-UPKO* (Ectopic expression of *Tg*EPT1-HA at the *TgUPRT* gene locus)
*Tg*EPT1-HA-R (PacI)	CTCATCTTAATTAATCAAGCGTAATCTGGAACATCGTATGGG	
*Tg*EPT2-F (NsiI)	CTCATCATGCATATGGTGTTTGGACACTACATTCCCCC	*pTgGRA2-UPKO* (Ectopic expression of *Tg*EPT2-HA at the *TgUPRT* gene locus)
*Tg*EPT2-HA-R (PacI)	CTCATCTTAATTAATCAAGCGTAATCTGGAACATCGTATGGG	

(21). The direct knock-out plasmid (*pTKO-TgPSD1mt-5′UTR-HXGPRT-TgPSD1mt-3′UTR*) consisted of 5′- and 3′-UTR elements (3 kb each) cloned at the KpnI/XhoI and HpaI/ApaI sites flanking the hypoxanthine xanthine guanine phosphoribosyltransferase (HXGPRT) resistance cassette (22). The vector was transfected into the Δ*ku80-hxgprt*$^-$ strain followed by transgenic selection using mycophenolic acid (25 μg/ml) and xanthine (50 μg/ml) (22). The drug-resistant parasites were cloned by limiting dilution and tested by crossover-specific PCR (primers in Table 1).

For 3′-insertional tagging (3′IT) of the *TgPSD1mt* gene with a C-terminal HA tag, its 1.3-kb crossover sequence fused to the epitope was amplified from tachyzoite gDNA and digested with XcmI and HpaI. It was cloned into XcmI/EcoRI-digested *pTKO-HXGPRT* vector, finally eliminating the EcoRI cloning site. The *pTKO-HXGPRT-TgPSD1mt-3′IT* construct was linearized by EcoRI present in the first half of the crossover sequence, transfected into the Δ*ku80-hxgprt*$^-$ strain (17), and then selected for HXGPRT expression, as described above. The resulting strain expressed *Tg*PSD1mt-HA under the control of its endogenous promoter and the *Tg*GRA2–3′UTR.

Immunofluorescence Microscopy—Parasite-infected HFF monolayers cultured on glass coverslips were washed with phosphate-buffered saline (PBS) at 24–30 h postinfection, fixed with 4% paraformaldehyde (10 min), and then neutralized with 0.1 M glycine, PBS (5 min). Cells were permeabilized with 0.2% Triton X-100, PBS for 20 min, and nonspecific binding was blocked with 2% bovine serum albumin in 0.2% Triton X-100, PBS (30 min). Samples were stained using anti-HA (1:1000; mouse), anti-*Tg*Gap45 (1:3000; rabbit), or anti-*Tg*F1B (1:1000; mouse) antibodies for 1 h. Cells were washed three times with 0.2% Triton X-100, PBS and stained with Alexa488- or Alexa594-conjugated antibodies (anti-rabbit or anti-mouse; 1:3000) for 45 min. Following three additional washing steps, samples were mounted in fluoromount G/DAPI (Southern-Biotech) and stored at 4 °C. Images were obtained using a Zeiss fluorescence microscope.

Immunoblot Analysis—Fresh extracellular tachyzoites (~3×10^7) were washed with PBS and pelleted (400 × *g*, 10 min, 4 °C). The parasite pellet was snap-frozen in liquid nitrogen and thawed in 10 mM MOPS/KOH buffer containing 250 mM sucrose and 1 mM EDTA (pH 7.2). The samples were probe-sonicated on ice (3× 30-s burst) followed by centrifugation (2000 × *g*, 5 min, 4 °C). The supernatant was centrifuged (30,000 × *g*, 1 h), and the resulting membrane pellet was suspended in 1% Triton X-100 and 2× sample loading buffer for SDS-PAGE. The immunoblot was probed with anti-HA (1:1000; rabbit; 2 h) or anti-*Tg*Hsp90 (1:1000; rabbit; 2 h) as primary antibody and HRP-conjugated anti-rabbit secondary (1:20,000; 1 h) antibody.

Tachyzoite Growth and Replication Assays—The growth fitness of tachyzoites was examined by plaque assays, recapitulating successive rounds of lytic cycles (*i.e.* invasion, replication, and egression). Confluent HFF cells in 6-well plates were infected with 200–400 parasites/well. The parasitized host cells were incubated in standard culture medium with 10% FCS for 7 days without perturbation (37 °C, 5% CO_2). Cells were washed twice with PBS, fixed with ice-cold methanol (2 min), and stained with crystal violet (10 min). To set up nutrient-depleted assays, normal FCS was replaced by dialyzed (PAA) or by lipid-depleted FCS (Biowest), as indicated, at the time of infection. The plaques were imaged and quantified using the ImageJ suite (National Institutes of Health, Bethesda, MD). To determine parasite replication, confluent HFF cells cultured on coverslips in 24-well plates were infected with tachyzoites (MOI = 1), incubated for 12–60 h, fixed, and then immunostained using anti-*Tg*Gap45 antibody (1:3000; rabbit). The mean numbers of parasites per vacuole were scored to compare the replication rates of the strains.

Yeast Complementation Assay—Yeast cells were grown in 2% yeast extract, 1% peptone, and 2% glucose or in synthetic uracil-free minimal medium (0.67% yeast nitrogen base; Difco) supplemented with appropriate amino acids and 2% glucose. The *S. cerevisiae psd1*Δ*psd2*Δ mutants (BY23480 and PTY44) were transformed with the constructs expressing *Tg*PSD1mt, *Tg*PSD1mtΔmtp, or *Sc*PSD1. The *Tg*PSD1mt and *Tg*PSD1mtΔmtp *Tg*PSD1mt$_{(91-427)}$ and *Tg*PSD1mt$_{(113-427)}$ cDNAs were cloned from parasite mRNA, and *Sc*PSD1 ORF was cloned from yeast gDNA (primers in Table 1). The ORFs were ligated into *pYES2.1* (Invitrogen) or *pESC-Ura* (Agilent Technologies) vectors expressing the *URA3* gene for selecting yeast transformants in uracil-deficient medium. Both plasmids allow galactose-inducible expression of a protein of interest under the control of the GAL promoter of *S. cerevisiae*.

Transformation was performed using standard yeast protocols. Transgenic cells were grown in synthetic uracil-dropout minimal medium supplemented with 2 mM ethanolamine and 2% glucose at 30 °C, and positive clones were identified by PCR and sequencing. For complementation assays, yeast cells were grown in liquid medium to an A_{600} of ~0.1, and serial dilutions (1:5) were stamped or spotted on synthetic uracil-dropout plates containing either glucose, galactose, or lactate (2%) with or without ethanolamine (2 mM). Plates were incubated for 2–3 days at 30 °C. For plasmid loss, yeast cells were serially propagated for 5 days under nonselective conditions (2% yeast extract, 1% peptone, and 2% glucose) and evaluated by replica plating on selective (uracil-free) and nonselective (uracil-replete) plates in synthetic minimal medium. They were also examined for their ability to grow with or without ethanolamine.

Subcellular Fractionation of S. cerevisiae—Yeast cells were grown to A_{600} = 0.4–0.8 in synthetic uracil-dropout medium supplemented with 2 mM ethanolamine and 2% galactose. All subsequent steps were performed at 4 °C. Cells were washed once with double-distilled H_2O and suspended in 50 mM potassium phosphate buffer (pH 6.8) containing EDTA (3 mM), phenylmethylsulfonyl fluoride (PMSF) (0.5 mM), and sucrose (0.25 M). Cell extract was prepared by disrupting yeast cells with glass beads (0.5-mm diameter) using a bead beater (Biospec Products) and removing the beads and cell debris by centrifugation (2000 × *g*, 5 min). Crude mitochondrial preparation was obtained by centrifuging cell extract (10,000 × *g*, 10 min) and two washes with buffer. The resulting supernatant was used to obtain the microsomes and cytosolic fractions (100,000 × *g*, 1 h). Yeast cells expressing *Sc*PSD1 (positive control) (10) were included to ascertain the efficiency of fractionation.

PtdSer Decarboxylase Assay—The reaction samples were prepared in 50 mM potassium phosphate (pH 6.8) buffer containing 10 mM β-mercaptoethanol, 0.25 M sucrose, 0.5 mM PMSF, 1 mM EDTA, and standard protease inhibitors. PSD activity was determined by trapping $^{14}CO_2$ released from Ptd[1-^{14}C]Ser on filter paper saturated with 2 M KOH (23). Ptd[1-^{14}C]Ser was made from L-[1-^{14}C]serine and dioleoyl CDP-diacylglycerol using PtdSer synthase. PtdSer synthase was purified from *E. coli* strain JA-200 harboring the plasmid *pPS3155* as described previously (24). The assay was performed at 30 °C in 16 × 100-mm borosilicate tubes sealed with an airtight rubber septum holding the KOH-saturated filter paper. The 0.8-ml assay mixture contained 60 mM potassium phosphate (pH 6.8), 0.17 M sucrose, 0.35 mM PMSF, 2 mM EDTA, 0.5 mM 2-mercaptoethanol, 0.5 mM dioleoyl Ptd[U-^{14}C]Ser (0.1 μCi/μmol), and 0.1% (w/v) Triton X-100. The reactions were started with 0.2 ml of yeast fractions and terminated after 1 h by the addition of 0.5 ml of 0.25 M H_2SO_4, introduced through the rubber septum using a hypodermic needle. The emitted $^{14}CO_2$ was trapped for 1 h prior to recovering the filter paper for liquid scintillation spectrometry.

Metabolic Labeling of Extracellular Parasites—The purification of fresh host-free tachyzoites and metabolic labeling were performed as described before (4). Briefly, HFF cells were infected with tachyzoites (MOI = 3), and parasites were collected 42 h postinfection. Samples were maintained on ice throughout the parasite isolation procedure. Infected cells were passed twice through 27-gauge needles to release the parasites, followed by removal of host cell debris by centrifugation (30 × *g*, 5 min). Parasites in the supernatant were pelleted (2000 × *g*, 10 min) and washed twice with intracellular type medium containing 20 mM HEPES, 140 mM KCl, 10 mM NaCl, 2.5 mM $MgCl_2$, 5 mM glucose, 0.1 μM $CaCl_2$, 1 mM sodium pyruvate, 1 mM Mg-ATP, MEM vitamins, MEM amino acids, and nonessential amino acids (pH 7.4). Fresh axenic tachyzoites (5×10^7) were incubated with [1,2-^{14}C]ethanolamine (20–40 nCi/nmol) or [1-^{3}H]serine (1 μCi/nmol) in 1 ml of intracellular type medium in glass tubes (2 h, 37 °C) followed by lipid extraction and quantification of radiolabeled phospholipids.

Metabolic Labeling of Intracellular Parasites—To examine the scavenging of host-derived lipids by intracellular parasites, HFF cells cultured in T25 flasks were labeled with [1,2-^{14}C]-ethanolamine (5 μCi, 25 μM) in DMEM containing aforementioned additives and lipid-depleted FCS (24 h, 37 °C, 5% CO_2). Cells were then infected with tachyzoites (MOI = 2). Cultures were supplemented with a 200-fold excess of unlabeled ethanolamine (5 mM) at the time of infection to dilute the residual pool of radioactive ethanolamine in the host cell cytosol, if any. The parasitized cells were incubated (48 h, 37 °C, 5% CO_2), and the parasites were released using 27-gauge needles. Tachyzoites were washed twice with PBS, counted, and subjected to lipid extraction. Total radioactivity accumulated in parasite lipids was quantified to deduce the import of host phospholipids by the replicating tachyzoites.

Lipid Extraction and Measurements—Lipid extraction from *T. gondii* was performed using the Bligh and Dyer method (25). The chloroform phase containing lipids was either used for liquid scintillation spectrometry or dried under nitrogen gas stream and suspended in chloroform and methanol (9:1). Lipids were resolved by one-dimensional TLC on silica gel 60 plates in chloroform, methanol, and acetate (65:25:10, v/v/v). To achieve a higher resolution, they were separated twice in chloroform, ethanol, water, and triethylamine (30:35:7:35, v/v/v/v) (26). Lipids were visualized by iodine or 8-anilino-1-naphthalenesulfonic acid staining and/or by autoradiography. All lipids were identified based on their co-migration with standards and quantified by liquid scintillation counting or by phosphorus assay (27).

Bioinformatics and Data Analyses—Initial identification of the parasite gene sequences was performed using the *Toxoplasma* genome database (ToxoDB) (28). *Tg*PSD1mt ORF was experimentally annotated by PCR and sequencing, and submitted to the NCBI database (accession number DQ450198). Prediction of the mitochondrial targeting peptide was done using MitoprotII (29), and the CLC sequence viewer was used for the protein alignment. For phylogenetic analysis, protein sequences were aligned based on the PFAM hidden Markov models (PF02666) using hmmer3 (30), and sequences were trimmed using trimAl (31). The phylogenetic tree was built using PhyML (32) and the LG model for amino acid substitution. Data plotting and statistical analyses were performed using the GraphPad Prism suite. Assays were performed at least three times unless specified otherwise. The error bars show the S.E. The statistical analyses were done using Student's *t* test, analysis of variance, and Bonferroni's test (*, $p < 0.05$; **, $p < 0.01$; ***, $p < 0.001$).

RESULTS

TgPSD1mt Is a Type I PtdSer Decarboxylase Localized in the Parasite Mitochondrion—Our earlier studies characterized a partially soluble PSD enzyme in *T. gondii*, which is secreted into the parasitophorous vacuole (*Tg*PSD1pv) via dense granules (13). This work and subsequent database mining also indicated the presence of a second PSD gene in the parasite (ToxoDB; TGGT1_225550). We cloned its ORF (427 residues), which contains a PtdSer decarboxylase domain (184–408 amino acids, Pfam domain PF02666) and a conserved LGST motif, required for the maturation and activity of PSD enzymes (Fig. 1*A*, *dotted red box*). *In silico* analysis of the protein sequence using MitoProtII predicted a high (98.5%) probability of import into the mitochondrion and a cleavage site between Ala-96 and Ser-97 (Fig. 1*A*, *green box*), which was confirmed by localization assays shown below. Hence, we named the protein *Tg*PSD1mt (*T. g*ondii PtdSer decarboxylase 1 mitochondrial).

Alignment of *Tg*PSD1mt with *P. falciparum* and human orthologs revealed a fairly high conservation, particularly in the PSD domain (Fig. 1*A*). *Tg*PSD1mt is 40% identical (62% similar) to *Pf*PSD and 35% identical (51% similar) to *Hs*PSD. The PSD proenzymes in prokaryotes as well as in eukaryotes are proteolytically processed between the Gly and Ser residues into a membrane-anchored β-subunit and a smaller α-subunit harboring the pyruvoyl moiety at its N terminus (33, 34). The pyruvoyl prosthetic group is part of the active site and is needed for the catalytic function of PSD enzymes. A similar processing of *Tg*PSD1mt is predicted to yield a mature protein with an ~32-kDa β-subunit and ~6-kDa α-subunit (see below; Fig. 5*E*). Phy-

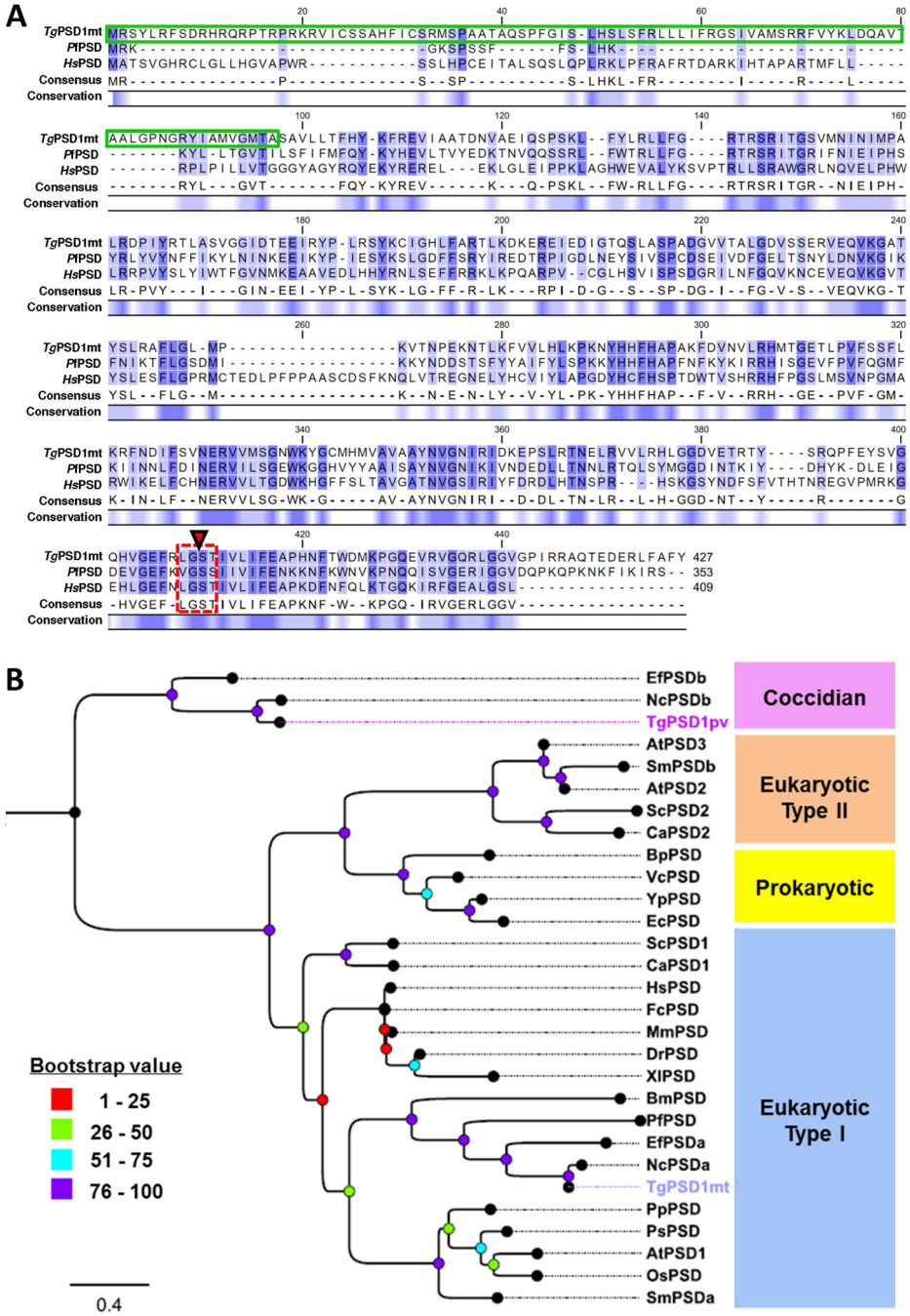

FIGURE 1. ***T. gondii* harbors two distinct phosphatidylserine decarboxylases, TgPSD1mt and TgPSD1pv.** *A*, alignment of PSD sequences from *T. gondii* (*Tg*PSD1mt), *P. falciparum* (*Pf*PSD), and *H. sapiens* (*Hs*PSD). Entirely and partly conserved residues are shown in *dark* and *light blue*, respectively. The *green* and *red boxes* represent the predicted mitochondrial targeting peptide and conserved cleavage motif at the catalytic site. The PSD domain in *Tg*PSD1mt spans residues 184–408 (Pfam domain, PF02666). *Tg*PSD1mt and *Pf*PSD have extended C termini. NCBI accession numbers are as follows: *Tg*PSD1mt, DQ450198; *Pf*PSD, XP_001352149; *Hs*PSD, Q9UG56. *B*, the phylogenetic clades of *Tg*PSD1mt, *Tg*PSD1pv, and orthologs. Branch support was estimated by 100 bootstrap replicates. *At*PSD1, *Arabidopsis thaliana* (GI 42566885); *At*PSD2, *A. thaliana* (GI 240256448); *At*PSD3 *A. thaliana* (GI 186513660); *Bm*PSD, *Babesia microti* (GI 399218717); *Bp*PSD, *Bordetella pertussis* (GI 33592417); *Ca*PSD1, *Candida albicans* (GI 68473808); *Ca*PSD2, *C. albicans* (GI 68468048); *Dr*PSD, *Danio rerio* (GI 63102372); *Ec*PSD, *E. coli* (GI 15804752); *Ef*PSDa, *Eimeria falciformis* (unpublished); *Ef*PSDb, *E. falciformis* (unpublished); *Fc*PSD, *Felis cattus* (GI 410976945); *Mm*PSD, *Mus musculus* (GI 74195621); *Nc*PSDa, *Neospora caninum* (GI 401409734); *Nc*PSDb, *N. caninum* (GI 401408937); *Os*PSD, *Oryza sativa* (GI 115450115); *Pf*PSD, *Pp*PSD, *Physcomitrella patens* (GI 168030155); *Ps*PSD, *Picea sitchensis* (GI 116788855); *Sc*PSD1, *S. cerevisiae* (GI 6324160); *Sc*PSD2, *S. cerevisiae* (GI 841244); *Sm*PSDa, *Selaginella moellendorffii* (GI 302802812); *Sm*PSDb, *S. moellendorffii* (GI 302818837); *Vc*PSD, *Vibrio cholera* (GI 446280068); *Xl*PSD, *Xenopus laevis* (GI 148236972); *Yp*PSD, *Yersinia pestis* (GI 22124534).

logenetic clustering showed that *Tg*PSD1mt belongs to the type I class PSD enzymes and is distinct from the previously described *Tg*PSD1pv protein (Fig. 1*B*). Our database searches also identified only one PSD in most protozoan parasites (not shown) except for a small subgroup of coccidians (*Eimeria* and *Neospora*), which express two discrete PSD enzymes related to *Tg*PSD1mt and *Tg*PSD1pv (Fig. 1*B*).

To determine the subcellular location of *Tg*PSD1mt in *T. gondii*, we generated stable transgenic parasites by 3′-HA tagging of the gene, which subsequently expressed

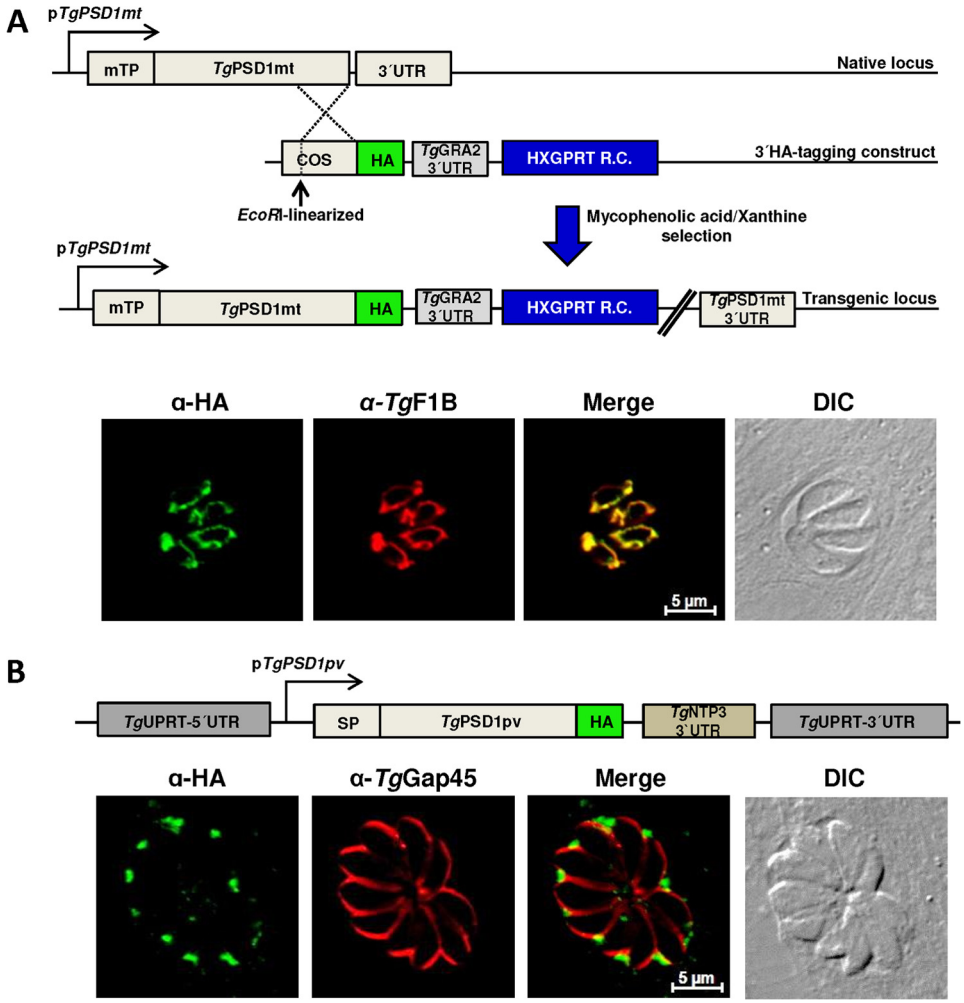

FIGURE 2. **TgPSD1mt localizes in the mitochondrion, whereas TgPSD1pv localizes in the parasitophorous vacuole of *T. gondii*.** *A*, epitope tagging of the *TgPSD1mt* gene and immunofluorescence imaging of intracellular parasites expressing *Tg*PSD1mt-HA under the control of its endogenous promoter. The construct for 3′-HA tagging of *Tg*PSD1mt (*pTKO-HXGPRT-TgPSD1mt-3′IT*) was transfected and selected in the Δ*ku80-hxgprt*$^{-}$ strain. Parasitized cells were stained with anti-HA and anti-*Tg*F1B antibodies after 24 h of infection. *B*, intracellular parasites stained for *Tg*PSD1pv-HA expression under the control of its native promoter via the *UPRT* locus (30-h infection). The parasite periphery is stained by anti-*Tg*Gap45 antibody. *COS*, crossover sequence; *mTP*, mitochondrial targeting peptide; *R.C.*, resistance cassette; *SP*, signal peptide.

*Tg*PSD1mt-HA under the control of its native promoter (Fig. 2*A*). Immunostaining of the intracellular parasites showed a mitochondrial localization of *Tg*PSD1mt-HA (*green*), which co-localized with a known organelle marker (*red*; *Tg*F1B) (15). Consistently, the enzyme was localized in the parasite mitochondrion when it was ectopically expressed under the control of a foreign promoter (see below; Fig. 5*D*). In contrast, *Tg*PSD1pv, regulated by its endogenous promoter, was localized in the parasitophorous vacuole (Fig. 2*B*) (13). These data reveal two phylogenetically distinct PSD enzymes in *T. gondii*, one of which is secreted into the parasitophorous vacuole (*Tg*PSD1pv), and a second one that is expressed in the parasite mitochondrion (*Tg*PSD1mt).

*TgPSD1mt Can Functionally Complement a psd1*Δ*psd2*Δ *Yeast Mutant*—To examine whether *Tg*PSD1mt is a functional PSD enzyme, we expressed the parasite protein in an *S. cerevisiae psd1*Δ*psd2*Δ mutant (Fig. 3). Ablation of the two native PSD proteins makes the yeast strains auxotrophic for ethanolamine, which is used to synthesize PtdEtn via the three-step CDP-ethanolamine pathway, of which the final reaction is located in the endoplasmic reticulum (Fig. 3*A*) (35). We expressed *Tg*PSD1mt cDNA under the regulation of the *ScGAL10* promoter in the *psd1*Δ*psd2*Δ yeast mutants. Empty vector and *Sc*PSD1 expression plasmid served as negative and positive controls, respectively (Fig. 3*B*). As expected, all transgenic yeast strains were able to grow under ethanolamine-replete conditions. The empty vector (negative) control did not show any detectable growth in ethanolamine-free medium, whereas *Tg*PSD1mt and *Sc*PSD1 rescued growth of the mutant in a galactose-inducible manner. To validate the specificity of complementation, we allowed yeast cells to lose the plasmid in nonselective medium. Cells that lost the PSD expression construct also lost their ability to grow on uracil-dropout selective plates as well as in ethanolamine-deficient nonselective medium (not shown).

Next, we produced subcellular fractions of the transgenic yeast strains to determine the distribution of *Tg*PSD1mt activity in the mitochondrial, microsomal, and cytosolic fractions. A *psd2*Δ yeast strain (JSY9750), expressing only the native *Sc*PSD1 in the mitochondria, was included to ascertain a suc-

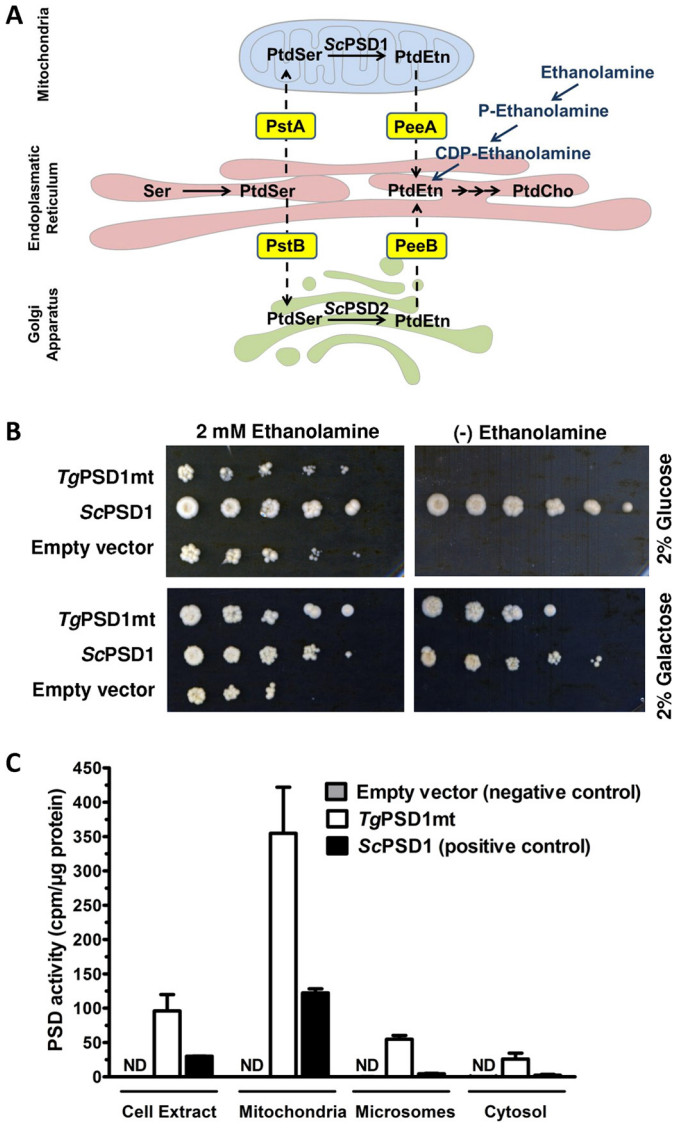

FIGURE 3. **TgPSD1mt can rescue the growth of an *S. cerevisiae* mutant lacking its endogenous PSD activity.** *A*, scheme of phospholipid synthesis in *S. cerevisiae*. Yeast harbors two PSD enzymes, *Sc*PSD1 and *Sc*PSD2, to produce PtdEtn from PtdSer in its mitochondria and the Golgi apparatus, respectively. The last reaction of the three-step CDP-ethanolamine pathway to synthesize PtdEtn is located in the ER. Exchange of PtdSer and PtdEtn between the organelles requires membrane contact sites and lipid transfer proteins (PstA/B and PeeA/B; adapted from Ref. 35). *B*, yeast complementation by heterologous expression of *Tg*PSD1mt in *S. cerevisiae psd1*Δ*psd2*Δ mutant (BY23480). *Tg*PSD1mt was expressed under the control of the *ScGAL10* promoter. Empty *pESC-Ura* and *Sc*PSD1 expression vectors were included as negative and positive controls. *C*, PSD activity in subcellular fractions of the yeast strains expressing *Tg*PSD1mt or endogenous *Sc*PSD1 or harboring empty vector. The indicated organelle-enriched fractions were subjected to PSD enzyme assays as described under "Materials and Methods." *ND*, not detectable. *Error bars*, S.E.

cessful fractionation (Fig. 3*C* (10, 12)). Each fraction was used to perform PSD assays by trapping $^{14}CO_2$ released by decarboxylation of radioactive PtdSer. As anticipated, the *psd1*Δ*psd2*Δ mutant harboring the empty vector did not show any measurable activity, and overexpression of *Tg*PSD1mt via the *ScGAL10* promoter was quite evident when compared with the positive control. Similar to *Sc*PSD1 (10, 12), a majority of the recovered *Tg*PSD1mt activity (>80%) was expressed in the mitochondria-enriched fraction.

The Mitochondrial Targeting Peptide in TgPSD1mt Is Required for Localization but Not for Activity—We next tested the importance of the predicted mitochondrial targeting peptide for localization and enzymatic activity. We expressed two HA-tagged deletion variants of *Tg*PSD1mt lacking the N-terminal peptide (*Tg*PSD1mt$_{(91-427)}$-HA and *Tg*PSD1mt$_{(113-427)}$-HA). None of the two truncated forms were localized in the parasite mitochondrion, and they displayed a diffuse fluorescence throughout the parasite instead (Fig. 4*A*). We also expressed *Tg*PSD1mt$_{(113-427)}$ in the yeast mutant to test the role of the N-terminal sequence for the catalytic activity and subcellular distribution. Notably, the truncated PSD was catalytically active and functionally complemented yeast growth in ethanolamine-free cultures (Fig. 4*B*), although only ~17% of the *Tg*PSD1mt$_{(113-427)}$ activity was present in the mitochondria-enriched fraction (Fig. 4*C*). These assays demonstrate that the N-terminal peptide is required for mitochondrial targeting but not for the catalytic function of *Tg*PSD1mt.

TgPSD1mt Is Dispensable for the Parasite Survival—Our further work focused on examining the physiological significance of *Tg*PSD1mt for *T. gondii*. Hence, we generated a tetracycline-regulatable conditional mutant in the Δ*ku80-TaTi* tachyzoites (Fig. 5*A*). To this end, we first ectopically expressed a tetracycline-repressible *Tg*PSD1mt-HA ORF (*Tg*PSD1mt-HA$_r$) at the *TgUPRT* locus. Then the merodiploid strain expressing *Tg*PSD1mt-HA$_r$ was subjected to the deletion of the *TgPSD1mt* locus by double homologous recombination. The mutant strain lacking the *TgPSD1mt* gene showed PCR bands specific for 5′- and 3′-crossovers (Fig. 5*B*). Subsequent DNA sequencing confirmed the successful recombination events. Finally, the Δ*tgpsd1mt*/*Tg*PSD1mt-HA$_r$ mutant showed a regulation of *Tg*PSD1mt mRNA by anhydrotetracycline (Fig. 5*C*), verifying the conditional nature of the strain.

In agreement with the above data, *Tg*PSD1mt-HA was localized in the mutant's mitochondrion and displayed a significant expression in the *on state* (no anhydrotetracycline) cultures (Fig. 5*D*). Its expression was markedly repressed by the drug within 1 day and disappeared after 3 days (*off state*). Immunoblot data confirmed a complete knockdown of *Tg*PSD1mt-HA in the conditional strain treated with the drug for one (2 days) or two (4 days) passages (Fig. 5*E*). The presence of three distinct drug-repressible bands, probably corresponding to preproenzyme, proenzyme, and α-subunit, indicated proteolytic maturation of *Tg*PSD1mt. The mutant could be cultured in the *off state* for a prolonged duration, which implied a nonessential nature of PSD. To further support the notion, we generated a knockout of *T. gondii* lacking the *TgPSD1mt* gene (Fig. 6*A*). The Δ*tgpsd1mt* mutant could be maintained in culture for multiple generations, which confirmed the expendable nature of *Tg*PSD1mt for the lytic cycle.

TgPSD1mt Is Required for an Optimal Parasite Growth and Replication—Following a successful genetic ablation of *Tg*PSD1mt, we examined the overall growth of the two mutants in human fibroblasts by performing plaque assays (36). The parasites were allowed to grow in host-cell monolayers for multiple rounds of lytic cycles (Fig. 6*B*). The plaques were evaluated for their numbers and area to assess the relative growth fitness of the knock-out and conditional mutants (Figs. 6*C* and 7*A* and

7*B*). The Δ*tgpsd1mt* strain exhibited an about 35% decrease in plaque size when compared with its parental strain (Fig. 6*C*). The Δ*tgpsd1mt*/*Tg*PSD1mt-HA$_r$ mutant displayed ~20% reduced plaque growth even in the absence of anhydrotetracycline (*on state*), which is probably due to a relatively weaker strength of the conditional promoter. A 7-day exposure to the drug accentuated the growth defect to 35% in the conditional mutant, whereas it had no apparent effect on the parental strain. Prolonged drug exposure for 10 days exerted a nearly 45% growth impairment in the conditional mutant (Fig. 7*B*). The plaque numbers for both mutants were similar to their respective parental strains (not shown). The average numbers of the parasites per vacuole during the course of infection confirmed that the observed growth defect is caused by an impaired replication of the mutant tachyzoites (Fig. 7*C*). These results reveal that *Tg*PSD1mt is needed for an optimal growth and replication of *T. gondii*, although it is dispensable for the parasite survival.

The TgPSD1mt Mutant Up-regulates the CDP-ethanolamine Pathway—For downstream assays, we used the Δ*tgpsd1mt*/*Tg*PSD1mt-HA$_r$ strain, which permitted a conditional testing (*on/off states*) and thus ensured the specificity of the stated observations. We first determined the phospholipid composition of parasites (Fig. 7*D*). Consistent with former results (4), phosphatidylcholine was the major lipid in the parental and mutant strains, followed by PtdEtn. Unexpectedly, no significant reduction in PtdEtn was apparent in the conditional mutant. The relative amounts of other major lipids were also unperturbed (Fig. 7*D*). These results prompted us to study the alternative routes of PtdEtn synthesis in the mutant. To discern a role of *Tg*PSD1pv, we performed metabolic labeling of parasite lipids with radioactive serine (Fig. 8*A*), which is mainly incorporated into PtdSer, and into PtdEtn following decarboxylation of the nascent PtdSer (4). Compared with the parental strain, only a modest (but statistically not significant) decline in lipid decarboxylation was detected despite a shutdown of *Tg*PSD1mt protein synthesis in the *off state* mutant (Fig. 5*E*). The data indicated a continual PtdEtn synthesis by decarboxylation of PtdSer in the mutant, which is probably due to *Tg*PSD1pv present in the dense granules (13).

The parasite is also known to produce PtdEtn from ethanolamine via the three-step CDP-ethanolamine pathway (4); its subcellular location in *T. gondii* is not defined so far. We found two putative EPT proteins in the parasite (ToxoDB; TGGT1_261760 and TGGT1_257510), which could catalyze the third and final step of PtdEtn synthesis (the transfer of phosphoethanolamine to diacylglycerol). Both *Tg*EPT1-HA and *Tg*EPT2-HA proteins co-localized with a known ER marker, *Tg*Der1-GFP (Fig. 8*B*) (18). To test whether the ER-derived lipid can alleviate depletion of the mitochondrial PtdEtn, we executed labeling of parasite lipids with radioactive ethanolamine (Fig. 8, *C* and D). As expected, ethanolamine was primarily incorporated into PtdEtn and into phosphoethanolamine-ceramide, as deduced by their TLC migration with the lipid standards. Ethanolamine metabolism was not affected by anhydrotetracycline in the parental strain, whereas the mutant in its *on state* showed a modest increase in the nascent PtdEtn (Fig. 8*C* and *D*). The *off state*

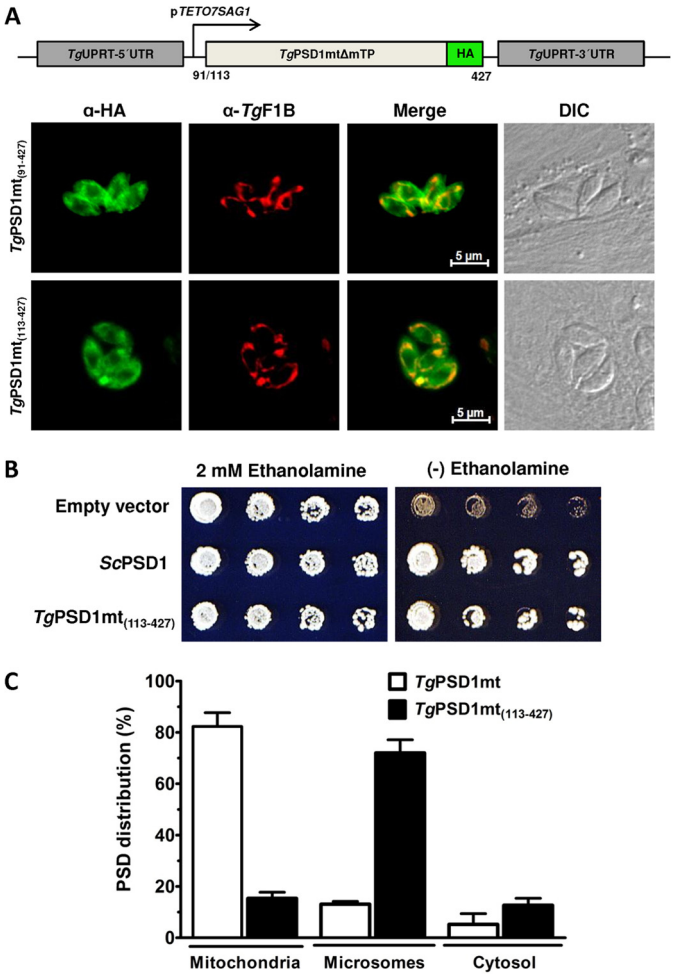

FIGURE 4. **The mitochondrial targeting peptide in TgPSD1mt is required for an efficient localization but not for enzyme activity.** *A*, immunofluorescence imaging of the two truncated HA-tagged *Tg*PSD1mt forms (*Tg*PSD1mt$_{(91-427)}$-HA and *Tg*PSD1mt$_{(113-427)}$-HA) expressed in *T. gondii* tachyzoites under the control of the *TETO7SAG1* promoter. Intracellular parasites were stained using anti-HA and anti-*Tg*F1B antibodies after 24 h of infection. *B*, complementation of *S. cerevisiae psd1*Δ*psd2*Δ mutant (PTY44) by *Tg*PSD1mt$_{(113-427)}$ in medium containing 2% lactate, 0.5% galactose. Empty *pYES2.1* and *Sc*PSD1-expressing vectors were used as negative and positive controls. *C*, enrichment of the PSD activity in subcellular fractions of yeast cells expressing *Tg*PSD1mt or *Tg*PSD1mt$_{(113-427)}$. *Error bars*, S.E.

mutant, on the other hand, utilized about 36% more substrate into PtdEtn than its own *on state* and showed 60–77% higher lipid labeling when compared with the parental strain (Fig. 8*D*). Collectively, these results demonstrate a sustained PtdSer decarboxylation as well as up-regulation of the CDP-ethanolamine route upon knockdown of mitochondrial PtdEtn synthesis.

The TgPSD1mt Mutant Can Tolerate a Depletion of Ethanolamine—To dissect the observed metabolic plasticity in *T. gondii*, we assessed whether the conditional mutant can survive simultaneous knockdown of *Tg*PSD1mt and depletion of ethanolamine in culture (Fig. 9*A*). To this end, we set up plaque assays using dialyzed FCS. As anticipated, the *Tg*PSD1mt mutant in the *on state* behaved similar to the parental strain, whereas in the *off state*, it exhibited an accentuated 56% growth defect that was partially restored by the addition of ethanolamine (Fig. 9*B*). A further inhibition of the mutant's growth,

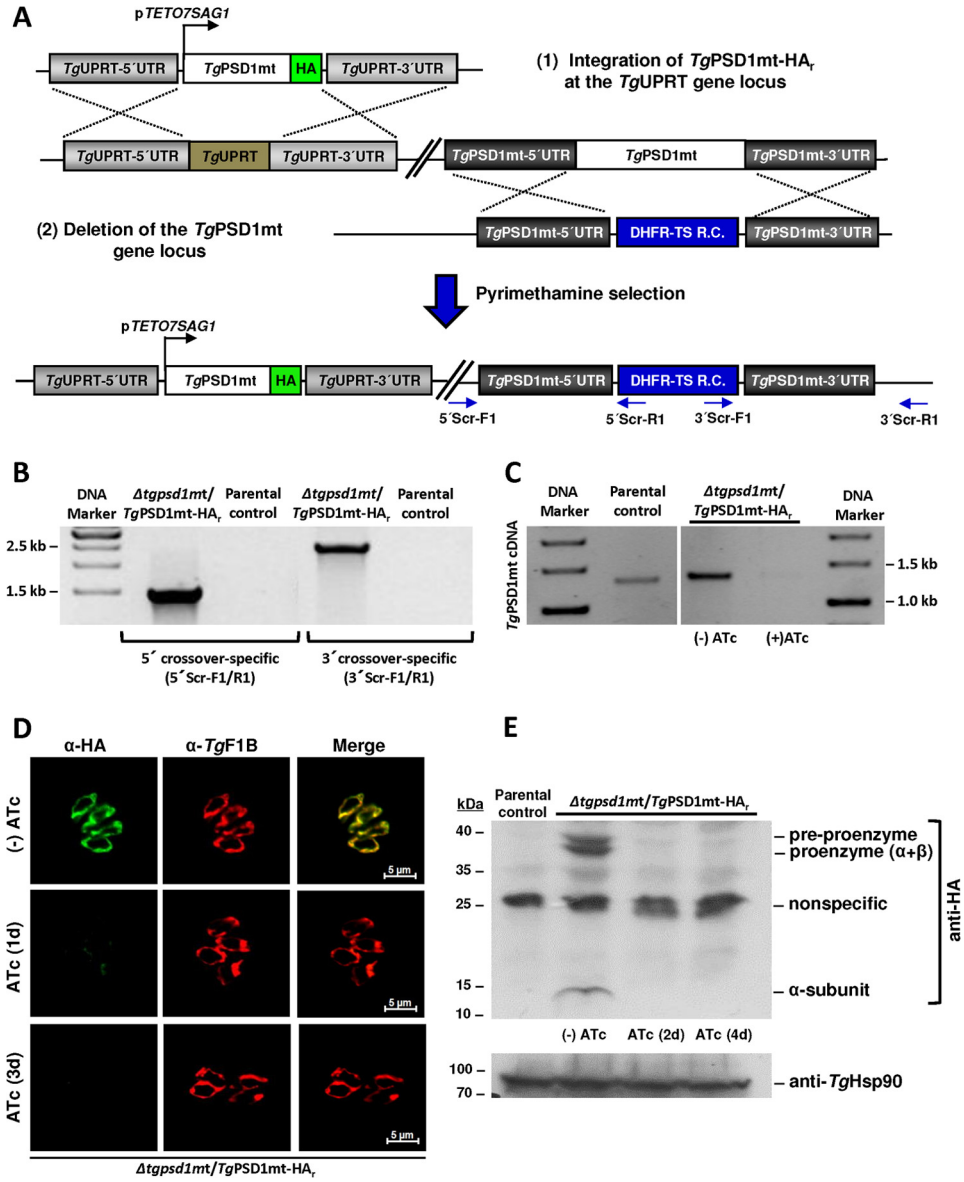

FIGURE 5. **Conditional mutagenesis allows a tetracycline-regulated knockdown of TgPSD1mt in *T. gondii*.** *A*, scheme for generating the Δ*tgpsd1mt/Tg*PSD1mt-HA$_r$ strain. A tetracycline-regulatable copy of *Tg*PSD1mt-HA was inserted at the *UPRT* locus, and the *TgPSD1mt* gene was deleted using a knock-out plasmid (*pTKO-TgPSD1mt-5′UTR-DHFR-TS-TgPSD1mt-3′UTR*). The primer pairs to screen for 5′- and 3′-recombination are depicted in *blue*. *B*, PCR testing of the Δ*tgpsd1mt/Tg*PSD1mt-HA$_r$ mutant. Pyrimethamine-resistant parasite clones were screened by genomic PCR using the 5′- and 3′-crossover-specific primers (5′Scr-F1/R1 and 3′Scr-F1/R1). The parental gDNA was included as a negative control. *C*, PCR analysis to verify the regulation of *Tg*PSD1mt mRNA by ATc. Total RNA isolated from the mutant or parental strain was used to generate cDNA and amplify *Tg*PSD1mt using ORF-specific primers. *D*, immunostaining of the mutant showing ATc-regulated expression of *Tg*PSD1mt-HA$_r$. The untreated control and drug-treated (1 and 3 days) parasites were stained using anti-HA and anti-*Tg*F1B antibodies (24-h infection). *E*, immunoblot image confirming the proteolytic processing and regulation of *Tg*PSD1mt-HA$_r$ protein in the conditional mutant. ATc treatment was performed for 2 or 4 days in cultures, and fresh host-free parasites were subjected to protein isolation and immunoblot analyses. Note that pre-proenzyme, proenzyme, and α-subunit of *Tg*PSD1mt-HA exhibit an aberrant migration in SDS-PAGE. A nonspecific band, which was not regulatable, was also observed in both strains. *Tg*Hsp90 (and nonspecific band) served as the loading control.

albeit modest, was observed when lipid-depleted serum was used in lieu of dialyzed FCS (Fig. 9*C*). The survival and resilient growth of the *off state* mutant in both serum types implied yet another route to drive PtdEtn biogenesis, potentially involving import of host-derived lipids. To test this, we first radioactively labeled the lipid pool in human fibroblasts and then allowed the conditional mutant to replicate and perform lipid biogenesis in prelabeled host cells (Fig. 9*D*). We measured a nearly 2-fold higher accumulation of radiolabeled lipid in the *off state* mutant. Although these data do not rule out a contribution of the CDP-ethanolamine pathway within the parasite, they are indicative of PtdEtn scavenging from the host cells when *de novo* synthesis by *Tg*PSD1mt is shut down. Taken together, our results also reveal a surprising level of metabolic plasticity in the parasite with respect to its growth and lipid biogenesis under varying nutrient conditions.

DISCUSSION

Here we show that *T. gondii* produces PtdEtn by decarboxylation of PtdSer, which is known to be synthesized via a base exchange type PtdSer synthase (4). The parasite harbors two phylogenetically distinct PSD proteins to synthesize PtdEtn,

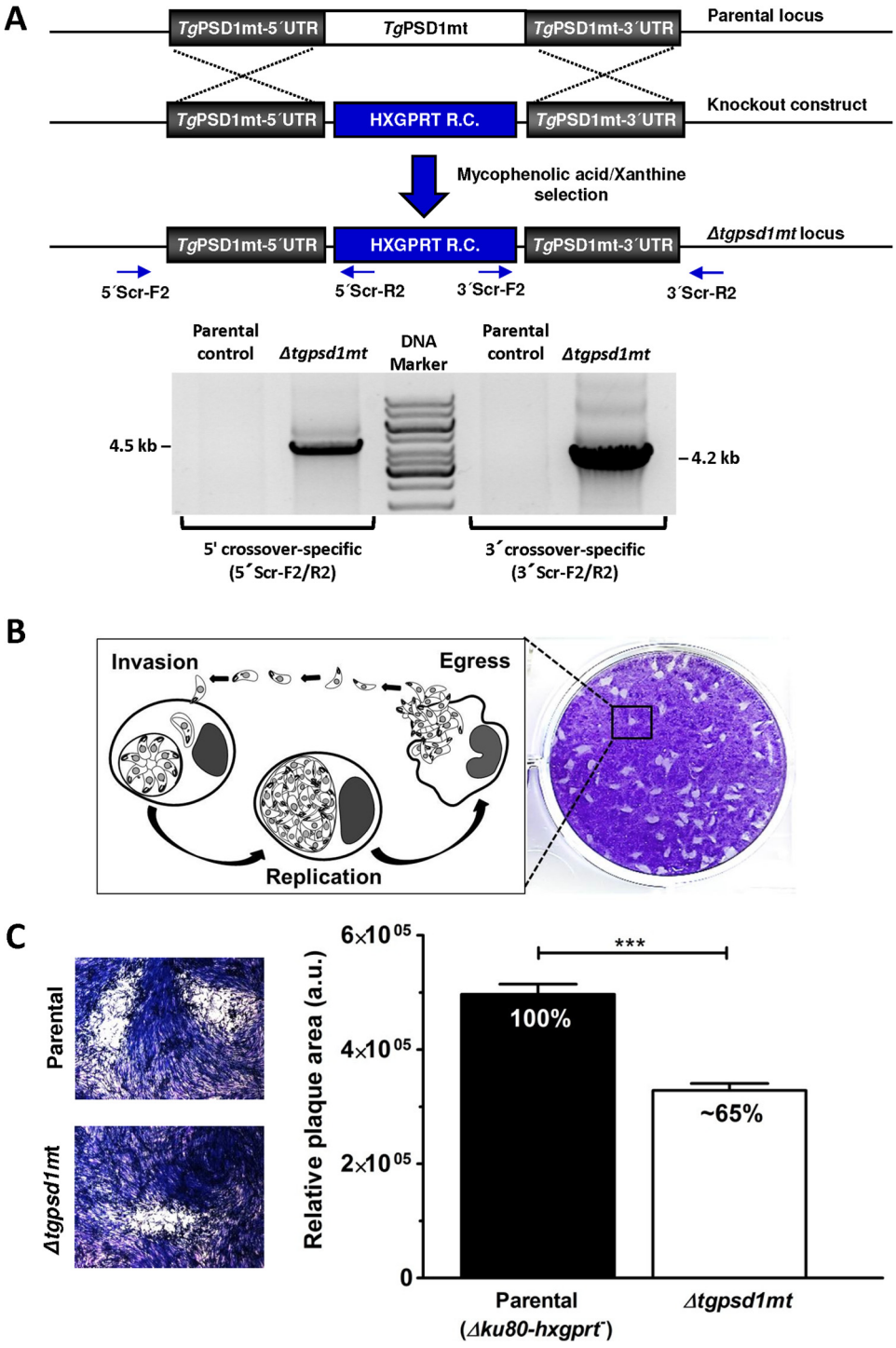

FIGURE 6. **TgPSD1mt is nonessential for survival but is required for efficient parasite growth.** *A*, scheme for generating the Δ*tgpsd1mt* strain. The *TgPSD1mt* gene was deleted using a knock-out construct (*pTKO-TgPSD1mt-5′UTR-HXGPRT-TgPSD1mt-3′UTR*). The Δ*tgpsd1mt* strain was confirmed by 5′ and 3′ PCR screening using the indicated primers (5′Scr-F2/R2 and 3′Scr-F2/R2). The parental gDNA was included as a negative control. *B*, schematized lytic cycle of *T. gondii* tachyzoites depicting the events of invasion, replication, and egression. Successive rounds of parasite cycles in confluent human fibroblasts over a 1-week period led to plaque formation. *C*, representative plaques formed by the Δ*tgpsd1mt* mutant and parental (Δ*ku80-hxgprt*$^-$) strains (*left*) and quantification of their sizes (*right*). In total, 200 plaques of each strain from three assays were measured for their area using the ImageJ software (***, $p < 0.001$). *Error bars*, S.E.

*Tg*PSD1mt and *Tg*PSD1pv, compartmentalized in the mitochondrion and parasitophorous vacuole, respectively. Most type I PSD enzymes localize in mitochondria except for *Pf*PSD1, which is reported to be expressed in the parasite ER (37). Unlike *Plasmodium* but consistent with mammalian, plant, and yeast cells (38–40), we demonstrate a typically conserved mitochondrial expression of *Tg*PSD1mt. *Plasmodium* and *Toxoplasma* also harbor the ethanolamine-dependent route to make PtdEtn in the parasite ER (4, 41). It therefore appears as if the synthesis of PtdEtn is confined to the endoplas-

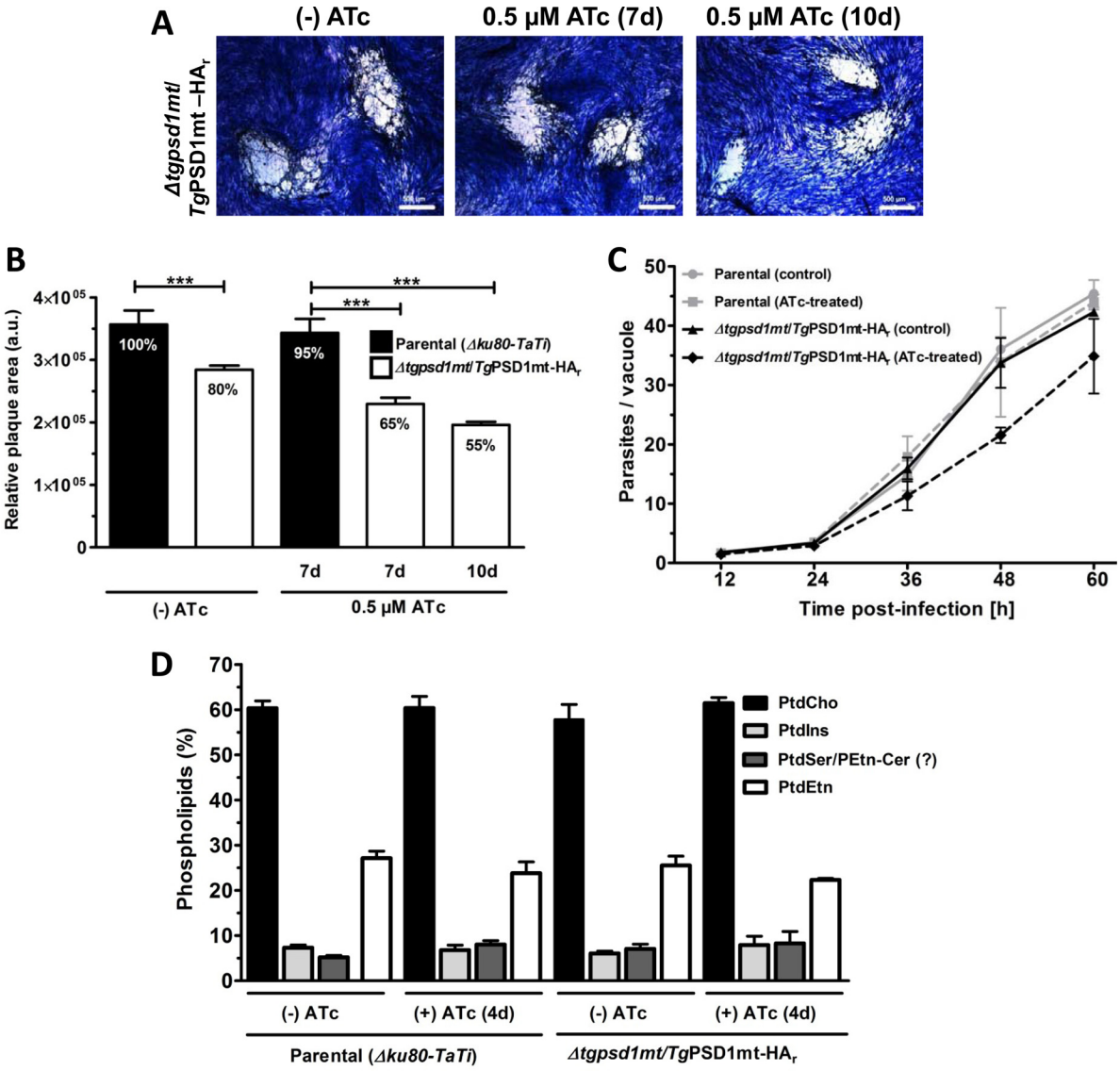

FIGURE 7. **The Δtgpsd1mt/TgPSD1mt-HA$_r$ mutant shows an impaired growth and replication despite a normal phospholipid composition.** *A*, representative plaques of the conditional mutant in the absence or presence of ATc (0.5 μM). For treatment exceeding 7 days, parasites were precultured with ATc. *B*, relative plaque areas of the strains from *A*. 200 plaques of each strain from three assays were quantified (***, $p < 0.001$). *C*, replication curves of the parental and mutant strains. For ATc treatment, parasites were cultured for three passages in drug-containing medium and used to infect human fibroblasts. Parasitized cells were stained with anti-*Tg*Gap45 antibody at the indicated time points. The average parasite numbers per vacuole were estimated by scoring 150 vacuoles from three assays. *D*, phospholipid composition of the parental and mutant strains. Lipids were resolved by one-dimensional TLC (chloroform, ethanol, water, triethylamine (30:35:7:35, v/v/v/v)) and then quantified by phosphorus assay. *Error bars*, S.E. PtdCho, phosphatidylcholine; PEtn-Cer, phosphoethanolamine-ceramide.

mic reticulum in *Plasmodium*, whereas this lipid is produced at multiple sites in *T. gondii* (*i.e.* mitochondrion, ER, parasitophorous vacuole, and dense granules (this work) (13)). Such an autonomous and resourceful PtdEtn synthesis bestows a considerable metabolic plasticity to *T. gondii* in differing nutritional niches.

The relative physiological significance of PtdSer decarboxylation and/or CDP-ethanolamine pathways varies among different organisms (8). For example, in the mouse, a deletion of mitochondrial PSD is embryonic lethal; however, ablation of ethanolamine-dependent lipid synthesis can be remunerated by PSD (42). The CDP-ethanolamine route is reported to be essential in protozoan parasites, *Plasmodium* and *Trypanosome* species (41, 43, 44). Conversely, *Arabidopsis* and *Saccharomyces* can tolerate a collective ablation of their PSD proteins or the CDP-ethanolamine pathway (11, 40). Interestingly, both of these routes are not mutually exclusive in *T. gondii*, and a specific lipid transfer appears to exist between the parasite mitochondrion and ER. Such an interorganelle lipid transport is reported to occur between the ER and mitochondria and/or the Golgi network in yeast (Fig. 3*A*), plants, and mammalian cells (45). The existence of such a process remains to be established in *T. gondii*.

The fact that *T. gondii* survives a concurrent knockdown of the *Tg*PSD1mt function and withdrawal of ethanolamine and lipids in culture implies additional routes for PtdEtn biogenesis, which involve *Tg*PSD1pv activity and lipid trafficking from the host organelles. This notion is supported by our data showing a continual synthesis of PtdEtn from PtdSer despite a knockdown of mitochondrial PSD and accrual of ethanolamine-derived

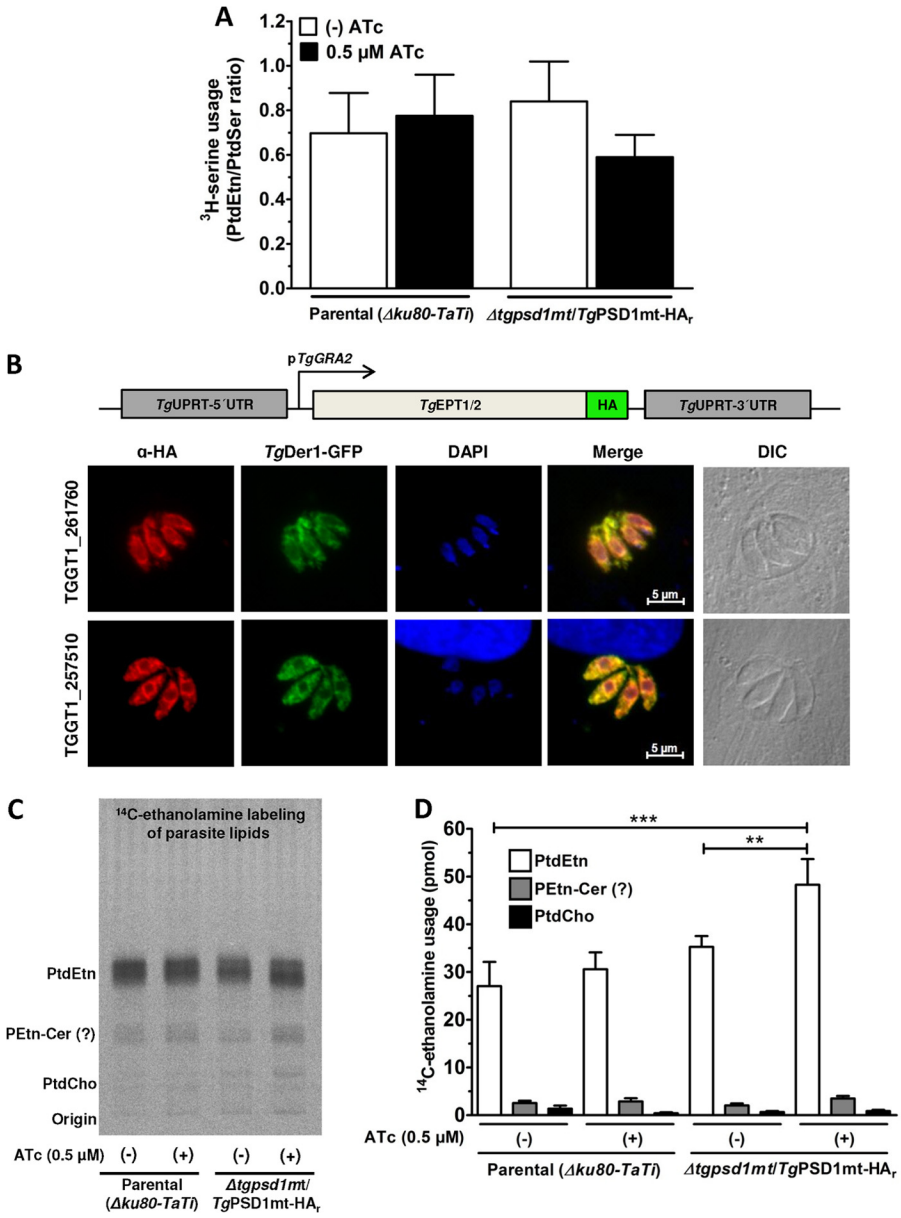

FIGURE 8. **PtdEtn synthesis in the endoplasmic reticulum is up-regulated upon knockdown of mitochondrial PSD in *T. gondii*.** *A*, labeling of parasite lipids with radioactive serine. Fresh extracellular parasites (5×10^7) of the parental or mutant strain (untreated or treated with ATc for two passages) were incubated with [^{3}H]serine (1 μCi/nmol, 2 h, 37 °C). Lipids were resolved by one-dimensional TLC (chloroform, methanol, acetate (65:25:10, v/v/v)) and subjected to liquid scintillation counting ($n = 3$ parental; $n = 5$ mutant). The differences between the conditions/strains are non-significant. *B*, immunolocalization of putative EPT enzymes (TGGT1_261760 and TGGT1_257510). The parasites were co-transfected with the vectors expressing *Tg*EPT1-HA or *Tg*EPT2-HA along with a *Tg*Der1-GFP expression plasmid and stained with anti-HA antibody after 24 h of infection. *C*, labeling of parasite lipids with radioactive ethanolamine. The parental or mutant parasites (5×10^7) were incubated with [^{14}C]ethanolamine (20–40 nCi/nmol, 2 h, 37 °C) followed by lipid isolation, TLC separation, and autoradiography. *D*, individual phospholipid bands from *C* were visualized by iodine vapor staining and scraped for scintillation counting ($n = 4$ assays; **, $p < 0.01$; ***, $p < 0.001$). *PEtn-Cer*, phosphoethanolamine-ceramide. *Error bars*, S.E.

host lipid(s) by intracellular parasites. It is known that the parasitophorous vacuole becomes associated with host mitochondria and ER (46), which are major sites of lipid synthesis in the mammalian cells (8, 45). This contiguous association of host organelles with the vacuole corresponds to the aforementioned zones of privileged lipid exchange, where PtdEtn and/or PtdSer may traffic to the parasite. Host-derived PtdSer could also be used to produce PtdEtn by *Tg*PSD1pv in the parasitophorous vacuole and dense granules. Akin to yeast and mammalian cells transporting PtdEtn/PtdSer across their membranes (47), the parasite genome harbors putative P4-ATPase permeases (ToxoDB), which may transport phospholipids across the vacuolar and plasma membranes in *T. gondii*. Finally, it was shown in *Leishmania* that degradation of sphingolipids by sphingosine 1-phosphate lyase can also contribute to PtdEtn synthesis (48). Our *in silico* analysis, however, did not reveal an ortholog in the *Toxoplasma* database.

It is an intriguing observation that *Tg*PSD1mt is not essential for the parasite survival but is required for optimal growth. In mammalian cells, ablation of PSD is often associated with fragmented/deformed and dysfunctional mitochondria (42, 49, 50). A knockdown of *Tg*PSD1mt, on the other hand, did not affect

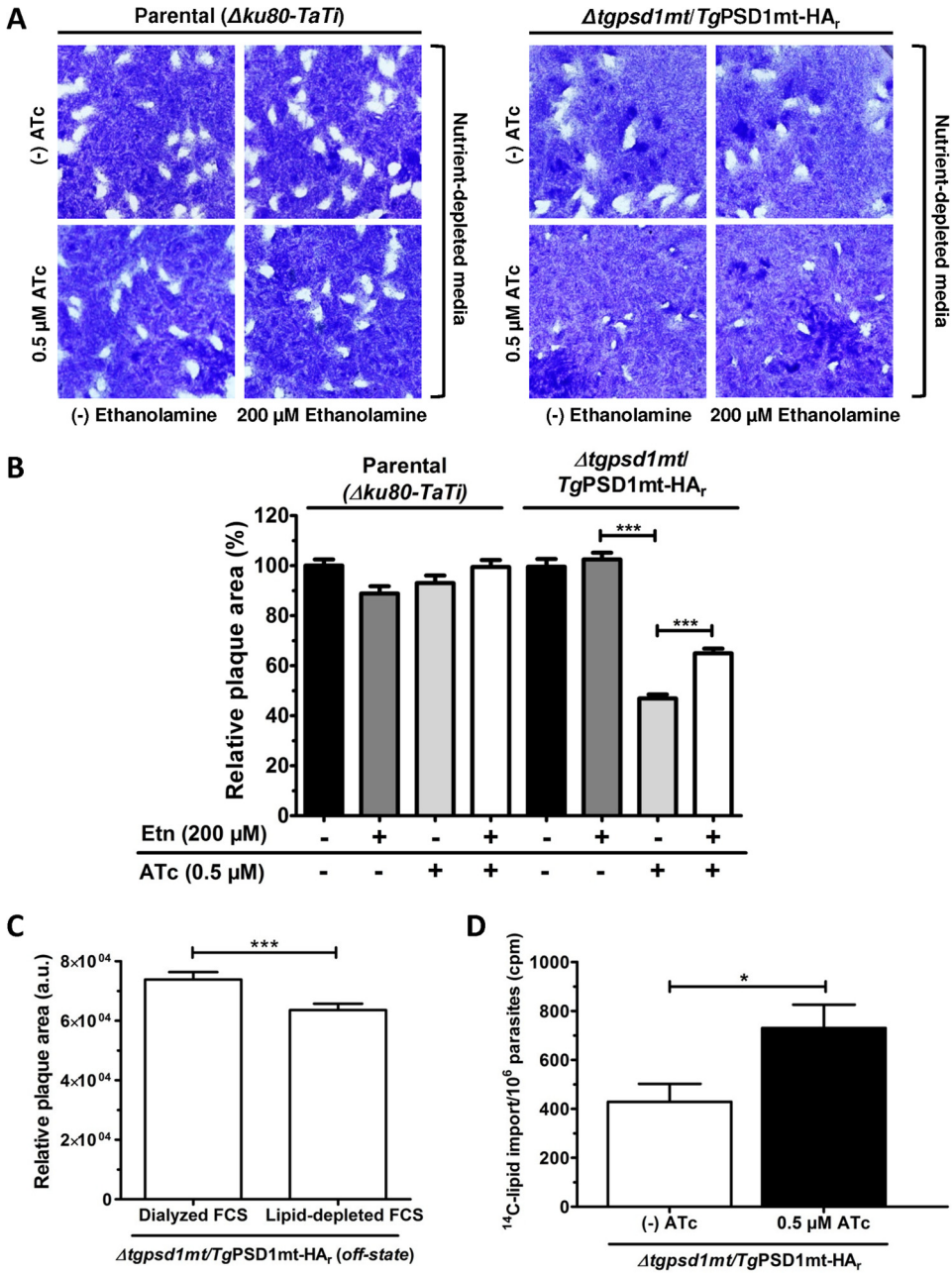

FIGURE 9. ***T. gondii* can survive a simultaneous knockdown of TgPSD1mt and depletion of ethanolamine.** *A*, representative plaques formed by the parental or Δ*tgpsd1mt*/*Tg*PSD1mt-HA$_r$ strains in the media containing dialyzed serum with or without ethanolamine supplementation. The *off state* parasites were pretreated for two passages with ATc, and treatment was maintained during plaque cultures. *B*, relative plaque areas of the parental and mutant strains from *A*. In total, 250 plaques of each strain or condition from three assays were quantified. *C*, plaques formed by the conditional mutant in medium supplemented with either dialyzed or lipid-depleted serum. *D*, accumulation of radioactive lipids in the conditional mutant following its intracellular replication in human fibroblasts labeled for PtdEtn prior to infection. Isotope labeling of host cells was performed with [^{14}C]ethanolamine (40 nCi/nmol) in medium containing lipid-depleted serum (24 h, 37 °C, 5% CO_2). Host cells were then infected with tachyzoites (MOI = 2; 48 h), as described under "Materials and Methods." Lipids isolated from fresh parasites were analyzed by liquid scintillation counting to estimate the import of host-derived lipids ($n = 4$ assays; *, $p < 0.05$; ***, $p < 0.001$). *Error bars*, S.E.

the typical lariat shape morphology of the organelle in *T. gondii* (Fig. 5*D*). Likewise, the import of a nucleus-encoded F1B-ATPase protein to the organelle was also unaltered in the Δ*tgpsd1mt*/*Tg*PSD1mt-HA$_r$ strain (Fig. 5*D*). Finally, the mitochondrial membrane potential showed no difference between the *on* and *off states*, as judged by quantifications of $DiOC_6$ fluorescence and by mitotracker staining of the parasite organelle (not shown). It is nonetheless plausible that the parasite makes exclusive PtdEtn species in the mitochondrion not produced otherwise, which may be needed for efficient parasite growth.

In conclusion, our work reveals that PtdEtn synthesis occurs at multiple distinct locations in *T. gondii*. The results suggest that synthesis of PtdEtn in this parasite parallels to the free living organisms, such as yeast and plant cells, and that PtdSer decarboxylation and the CDP-ethanolamine routes cooperate with each other. An interorganelle exchange of lipids ensures the parasite survival and growth in varying nutritional milieus.

Last but not least, *T. gondii* with its established genetic manipulation tools offers an instructive model to explore the lipid biology of intracellular pathogens.

Acknowledgments—We thank Grit Meusel, René Lang, and Vera Sampels (Humboldt University) for research assistance and Wayne Riekhof and Jae-Yeon Choi (National Jewish Health) for experimental guidance. We are also grateful to Maik Lehmann, Emanuel Heitlinger, and Thomas Korte (Humboldt University) for supporting microscopy, bioinformatics, and radioactivity work, respectively.

REFERENCES

1. Black, M. W., and Boothroyd, J. C. (2000) Lytic cycle of *Toxoplasma gondii*. *Microbiol. Mol. Biol. Rev.* **64,** 607–623
2. Sullivan, W. J., Jr., and Jeffers, V. (2012) Mechanisms of *Toxoplasma gondii* persistence and latency. *FEMS Microbiol. Rev.* **36,** 717–733
3. Coppens, I. (2013) Targeting lipid biosynthesis and salvage in apicomplexan parasites for improved chemotherapies. *Nature reviews. Microbiology* **11,** 823–835
4. Gupta, N., Zahn, M. M., Coppens, I., Joiner, K. A., and Voelker, D. R. (2005) Selective disruption of phosphatidylcholine metabolism of the intracellular parasite *Toxoplasma gondii* arrests its growth. *J. Biol. Chem.* **280,** 16345–16353
5. Sampels, V., Hartmann, A., Dietrich, I., Coppens, I., Sheiner, L., Striepen, B., Herrmann, A., Lucius, R., and Gupta, N. (2012) Conditional mutagenesis of a novel choline kinase demonstrates plasticity of phosphatidylcholine biogenesis and gene expression in *Toxoplasma gondii*. *J. Biol. Chem.* **287,** 16289–16299
6. Charron, A. J., and Sibley, L. D. (2002) Host cells. Mobilizable lipid resources for the intracellular parasite *Toxoplasma gondii*. *J. Cell Sci.* **115,** 3049–3059
7. Vance, J. E., and Tasseva, G. (2013) Formation and function of phosphatidylserine and phosphatidylethanolamine in mammalian cells. *Biochim. Biophys. Acta* **1831,** 543–554
8. Vance, J. E., and Vance, D. E. (2004) Phospholipid biosynthesis in mammalian cells. *Biochem. Cell Biol.* **82,** 113–128
9. Dowhan, W. (1997) Phosphatidylserine decarboxylases. Pyruvoyl-dependent enzymes from bacteria to mammals. *Methods Enzymol.* **280,** 81–88
10. Trotter, P. J., and Voelker, D. R. (1995) Identification of a non-mitochondrial phosphatidylserine decarboxylase activity (PSD2) in the yeast *Saccharomyces cerevisiae*. *J. Biol. Chem.* **270,** 6062–6070
11. Nerlich, A., von Orlow, M., Rontein, D., Hanson, A. D., and Dörmann, P. (2007) Deficiency in phosphatidylserine decarboxylase activity in the psd1 psd2 psd3 triple mutant of *Arabidopsis* affects phosphatidylethanolamine accumulation in mitochondria. *Plant Physiol.* **144,** 904–914
12. Trotter, P. J., Pedretti, J., and Voelker, D. R. (1993) Phosphatidylserine decarboxylase from *Saccharomyces cerevisiae*. Isolation of mutants, cloning of the gene, and creation of a null allele. *J. Biol. Chem.* **268,** 21416–21424
13. Gupta, N., Hartmann, A., Lucius, R., and Voelker, D. R. (2012) The obligate intracellular parasite *Toxoplasma gondii* secretes a soluble phosphatidylserine decarboxylase. *J. Biol. Chem.* **287,** 22938–22947
14. Gaskins, E., Gilk, S., DeVore, N., Mann, T., Ward, G., and Beckers, C. (2004) Identification of the membrane receptor of a class XIV myosin in *Toxoplasma gondii*. *J. Cell Biol.* **165,** 383–393
15. Besteiro, S., Brooks, C. F., Striepen, B., and Dubremetz, J. F. (2011) Autophagy protein Atg3 is essential for maintaining mitochondrial integrity and for normal intracellular development of *Toxoplasma gondii* tachyzoites. *PLoS Pathog.* **7,** e1002416
16. Sheiner, L., Demerly, J. L., Poulsen, N., Beatty, W. L., Lucas, O., Behnke, M. S., White, M. W., and Striepen, B. (2011) A systematic screen to discover and analyze apicoplast proteins identifies a conserved and essential protein import factor. *PLoS Pathog.* **7,** e1002392
17. Huynh, M. H., and Carruthers, V. B. (2009) Tagging of endogenous genes in a *Toxoplasma gondii* strain lacking Ku80. *Eukaryot. Cell* **8,** 530–539
18. Agrawal, S., van Dooren, G. G., Beatty, W. L., and Striepen, B. (2009) Genetic evidence that an endosymbiont-derived endoplasmic reticulum-associated protein degradation (ERAD) system functions in import of apicoplast proteins. *J. Biol. Chem.* **284,** 33683–33691
19. Meissner, M., Schlüter, D., and Soldati, D. (2002) Role of *Toxoplasma gondii* myosin A in powering parasite gliding and host cell invasion. *Science* **298,** 837–840
20. Donald, R. G., and Roos, D. S. (1995) Insertional mutagenesis and marker rescue in a protozoan parasite. Cloning of the uracil phosphoribosyltransferase locus from *Toxoplasma gondii*. *Proc. Natl. Acad. Sci. U.S.A.* **92,** 5749–5753
21. Donald, R. G., and Roos, D. S. (1993) Stable molecular transformation of *Toxoplasma gondii*. A selectable dihydrofolate reductase-thymidylate synthase marker based on drug-resistance mutations in malaria. *Proc. Natl. Acad. Sci. U.S.A.* **90,** 11703–11707
22. Donald, R. G., Carter, D., Ullman, B., and Roos, D. S. (1996) Insertional tagging, cloning, and expression of the *Toxoplasma gondii* hypoxanthine-xanthine-guanine phosphoribosyltransferase gene. Use as a selectable marker for stable transformation. *J. Biol. Chem.* **271,** 14010–14019
23. Dowhan, W., Wickner, W. T., and Kennedy, E. P. (1974) Purification and properties of phosphatidylserine decarboxylase from *Escherichia coli*. *J. Biol. Chem.* **249,** 3079–3084
24. Ohta, A., Waggoner, K., Radominska-Pyrek, A., and Dowhan, W. (1981) Cloning of genes involved in membrane lipid synthesis. Effects of amplification of phosphatidylglycerophosphate synthase in *Escherichia coli*. *J. Bacteriol.* **147,** 552–562
25. Bligh, E. G., and Dyer, W. J. (1959) A rapid method of total lipid extraction and purification. *Can. J. Biochem. Physiol.* **37,** 911–917
26. Vaden, D. L., Gohil, V. M., Gu, Z., and Greenberg, M. L. (2005) Separation of yeast phospholipids using one-dimensional thin-layer chromatography. *Anal. Biochem.* **338,** 162–164
27. Rouser, G., Fkeischer, S., and Yamamoto, A. (1970) Two dimensional thin layer chromatographic separation of polar lipids and determination of phospholipids by phosphorus analysis of spots. *Lipids* **5,** 494–496
28. Gajria, B., Bahl, A., Brestelli, J., Dommer, J., Fischer, S., Gao, X., Heiges, M., Iodice, J., Kissinger, J. C., Mackey, A. J., Pinney, D. F., Roos, D. S., Stoeckert, C. J., Jr., Wang, H., and Brunk, B. P. (2008) ToxoDB: an integrated *Toxoplasma gondii* database resource. *Nucleic Acids Res.* **36,** D553–D556
29. Claros, M. G. (1995) MitoProt, a Macintosh application for studying mitochondrial proteins. *Comput. Appl. Biosci.* **11,** 441–447
30. Eddy, S. R. (2011) Accelerated Profile HMM Searches. *PLoS Comput. Biol.* **7,** e1002195
31. Capella-Gutiérrez, S., Silla-Martínez, J. M., and Gabaldón, T. (2009) trimAl. A tool for automated alignment trimming in large-scale phylogenetic analyses. *Bioinformatics* **25,** 1972–1973
32. Guindon, S., Delsuc, F., Dufayard, J. F., and Gascuel, O. (2009) Estimating maximum likelihood phylogenies with PhyML. *Methods Mol. Biol.* **537,** 113–137
33. Horvath, S. E., Böttinger, L., Vögtle, F. N., Wiedemann, N., Meisinger, C., Becker, T., and Daum, G. (2012) Processing and topology of the yeast mitochondrial phosphatidylserine decarboxylase 1. *J. Biol. Chem.* **287,** 36744–36755
34. Kuge, O., Saito, K., Kojima, M., Akamatsu, Y., and Nishijima, M. (1996) Post-translational processing of the phosphatidylserine decarboxylase gene product in Chinese hamster ovary cells. *Biochem. J.* **319,** 33–38
35. Voelker, D. R. (2005) Bridging gaps in phospholipid transport. *Trends Biochem. Sci.* **30,** 396–404
36. Kim, K., and Weiss, L. M. (2014) *Toxoplasma gondii* the Model Apicomplexan, Perspectives and Methods. 2nd Ed., pp. 599–600, Academic Press, London, UK
37. Baunaure, F., Eldin, P., Cathiard, A. M., and Vial, H. (2004) Characterization of a non-mitochondrial type I phosphatidylserine decarboxylase in *Plasmodium falciparum*. *Mol. Microbiol.* **51,** 33–46
38. Percy, A. K., Moore, J. F., Carson, M. A., and Waechter, C. J. (1983) Characterization of brain phosphatidylserine decarboxylase. Localization in the mitochondrial inner membrane. *Arch. Biochem. Biophys.* **223,**

484–494
39. Rontein, D., Wu, W. I., Voelker, D. R., and Hanson, A. D. (2003) Mitochondrial phosphatidylserine decarboxylase from higher plants. Functional complementation in yeast, localization in plants, and overexpression in *Arabidopsis*. *Plant Physiol.* **132,** 1678–1687
40. Trotter, P. J., Pedretti, J., Yates, R., and Voelker, D. R. (1995) Phosphatidylserine decarboxylase 2 of *Saccharomyces cerevisiae*. Cloning and mapping of the gene, heterologous expression, and creation of the null allele. *J. Biol. Chem.* **270,** 6071–6080
41. Déchamps, S., Wengelnik, K., Berry-Sterkers, L., Cerdan, R., Vial, H. J., and Gannoun-Zaki, L. (2010) The Kennedy phospholipid biosynthesis pathways are refractory to genetic disruption in *Plasmodium berghei* and therefore appear essential in blood stages. *Mol. Biochem. Parasitol.* **173,** 69–80
42. Steenbergen, R., Nanowski, T. S., Beigneux, A., Kulinski, A., Young, S. G., and Vance, J. E. (2005) Disruption of the phosphatidylserine decarboxylase gene in mice causes embryonic lethality and mitochondrial defects. *J. Biol. Chem.* **280,** 40032–40040
43. Gibellini, F., Hunter, W. N., and Smith, T. K. (2009) The ethanolamine branch of the Kennedy pathway is essential in the bloodstream form of *Trypanosoma brucei*. *Mol. Microbiol.* **73,** 826–843
44. Signorell, A., Gluenz, E., Rettig, J., Schneider, A., Shaw, M. K., Gull, K., and Bütikofer, P. (2009) Perturbation of phosphatidylethanolamine synthesis affects mitochondrial morphology and cell-cycle progression in procyclic-form *Trypanosoma brucei*. *Mol. Microbiol.* **72,** 1068–1079
45. Osman, C., Voelker, D. R., and Langer, T. (2011) Making heads or tails of phospholipids in mitochondria. *J. Cell Biol.* **192,** 7–16
46. Sinai, A. P., Webster, P., and Joiner, K. A. (1997) Association of host cell endoplasmic reticulum and mitochondria with the *Toxoplasma gondii* parasitophorous vacuole membrane. A high affinity interaction. *J. Cell Sci.* **110,** 2117–2128
47. Pomorski, T., Holthuis, J. C., Herrmann, A., and van Meer, G. (2004) Tracking down lipid flippases and their biological functions. *J. Cell Sci.* **117,** 805–813
48. Zhang, K., Pompey, J. M., Hsu, F. F., Key, P., Bandhuvula, P., Saba, J. D., Turk, J., and Beverley, S. M. (2007) Redirection of sphingolipid metabolism toward de novo synthesis of ethanolamine in Leishmania. *EMBO J.* **26,** 1094–1104
49. Tasseva, G., Bai, H. D., Davidescu, M., Haromy, A., Michelakis, E., and Vance, J. E. (2013) Phosphatidylethanolamine deficiency in mammalian mitochondria impairs oxidative phosphorylation and alters mitochondrial morphology. *J. Biol. Chem.* **288,** 4158–4173
50. Chan, E. Y., and McQuibban, G. A. (2012) Phosphatidylserine decarboxylase 1 (psd1) promotes mitochondrial fusion by regulating the biophysical properties of the mitochondrial membrane and alternative topogenesis of mitochondrial genome maintenance protein 1 (mgm1). *J. Biol. Chem.* **287,** 40131–40139